

HIGH-PRESSURE AND HIGH-TEMPERATURE METAMORPHISM OF THE MAFIC AND ULTRAMAFIC LAC ESPADON SUITE, MANICOUAGAN IMBRICATE ZONE, EASTERN GRENVILLE PROVINCE, QUÉBEC*

RICHARD COX[§] AND APHRODITE INDARES

Department of Earth Sciences, Memorial University of Newfoundland, St John's, Newfoundland A1B 3X5

ABSTRACT

The Lac Espadon suite (LES) of the Manicouagan Imbricate Zone (Quebec) is comprised of layered mafic and ultramafic rocks, Labradorian in age (*ca.* 1650–1630 Ma) that were variably deformed and metamorphosed under high-pressure and high-temperature (high-PT) conditions during the Grenvillian Orogeny. Maximum P–T conditions of 780–930°C at 16–19 kbar (high-T eclogite facies) are recorded in massive coronitic troctolite and hornblende from the western part of the LES. In these rocks, metamorphic coronas of orthopyroxene, clinopyroxene and garnet have grown at the expense of igneous olivine and plagioclase. Relict plagioclase contains inclusions of kyanite and corundum, and garnet coronas locally preserve growth zoning. Deformed margins of the mafic rocks have granoblastic hydrous assemblages that are interpreted to have equilibrated during exhumation at *ca.* 700°C at 10–12 kbar and then down to *ca.* 600°C at 5 kbar (amphibolite-facies conditions), suggesting a steep retrograde P–T path. Olivine gabbro from the eastern part of the LES records peak conditions of 775–870°C at 14.5–16.25 kbar. Granoblastic areas in the rock are partially hydrated and give conditions of 760–820°C at 12–14 kbar, suggesting a near-isothermal P–T trajectory. The P–T paths are compatible with structural evidence suggesting tectonic exhumation of these rocks by northwesterly thrusting, with extension on top of the pile. The high-PT conditions and steep decompression paths recorded by the LES are similar to those in several adjacent and nearby terranes, suggesting widespread tectonic exhumation of the lower crust in this area of the Grenville Province.

Keywords: Grenville Province, mafic rocks, coronas, eclogite facies, amphibolite facies, Manicouagan, Quebec.

SOMMAIRE

La suite du lac Espadon, membre de la zone imbriquée de Manicouagan (Province du Grenville, Québec), contient des roches mafiques et ultramafiques stratiformes d'âge labradorien (environ 1650–1630 Ma) qui ont été plus ou moins déformées et métamorphosées à pression et à température élevées au cours de l'orogénèse grenvillienne. Les conditions du métamorphisme ont atteint 780–930°C à 16–19 kbar (faciès éclogite de haute température), comme en témoignent la troctolite et la hornblende coronitiques massives du secteur ouest de cette unité. Dans ces roches, les textures coronitiques impliquant orthopyroxène, clinopyroxène et grenat se sont développées aux dépens de l'olivine et du plagioclase primaires. Les reliques de plagioclase contiennent des inclusions de kyanite et de corindon, et les couronnes de grenat conservent ici et là une zonation due à la croissance. Les bordures déformées des massifs mafiques contiennent des assemblages granoblastiques de minéraux hydratés qui témoigneraient d'un ré-équilibre au cours d'une exhumation sur l'intervalle 700°C et 10–12 kbar jusqu'à environ 600°C à 5 kbar (conditions du faciès amphibolite), indication d'une évolution P–T rétrograde abrupte. Le gabbro à olivine du secteur oriental de cette unité a subi un métamorphisme jusqu'à 775–870°C et 14.5–16.25 kbar. Les portions à texture granoblastique ont été partiellement hydratées à 760–820°C et 12–14 kbar, ce qui fait penser à une trajectoire P–T quasiment isotherme. Les tracés P–T sont compatibles avec l'évidence structurale d'une exhumation tectonique de ces roches au cours d'un chevauchement vers le nord-ouest, accompagné d'une extension des parties supérieures de l'empilement. Les conditions de pression et de température élevées et la décompression abrupte sont semblables aux conditions déduites dans les socles adjacents ou voisins, ce qui indique une exhumation répandue de la croûte inférieure dans cette région de la Province du Grenville.

Mots-clés: Province du Grenville, roches mafiques, couronnes, faciès éclogite, faciès amphibolite, Manicouagan, Québec.

* LITHOPROBE contribution number 1049

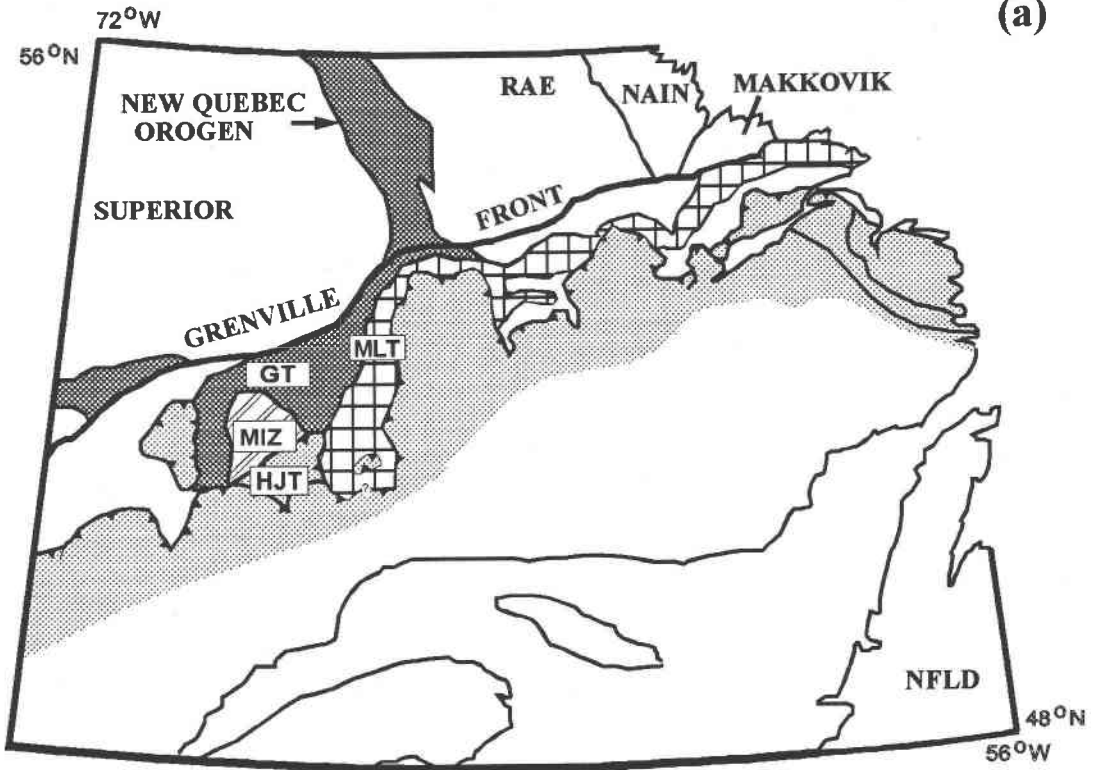
§ E-mail address: rcox@sparky2.esd.mun.ca

INTRODUCTION

High-grade metamorphic terranes constitute petrological windows through which processes in the deep crust in orogenic belts can be studied. In such terranes, rocks in which metamorphic reactions have not gone to completion may allow segments of their pressure and temperature (P-T) history to be recovered. Rocks with corona textures are especially suitable for studies of this type, and may be regarded as displaying local or domainal equilibrium (Rubie 1990). The best examples of such textures are commonly found in coarse-grained, dry and relatively undeformed, mafic (meta-igneous) rocks (e.g., Mørk 1985, 1986, Pognante 1985, Koons *et al.* 1987, Rivers & Mengel 1988, Indares 1993, Indares & Rivers 1995). In contrast, their deformed equivalents commonly display granoblastic textures due to enhanced chemical diffusion and fluid infiltration from country rocks (e.g., Heinrich 1982, Rubie 1986, Koons *et al.* 1987). The result is that coronitic rocks at the cores of igneous bodies commonly record near-peak conditions of metamorphism better than their recrystallized margins, as the latter are also more readily retrograde, again due to the presence of fluid that allows the development of hydrous phases at amphibolite-facies conditions. Application of thermobarometry to coronitic rocks is particularly difficult because the presence of coronas suggests global disequilibrium. However, a detailed

al. 1987, Rivers & Mengel 1988, Indares 1993, Indares & Rivers 1995). In contrast, their deformed equivalents commonly display granoblastic textures due to enhanced chemical diffusion and fluid infiltration from country rocks (e.g., Heinrich 1982, Rubie 1986, Koons *et al.* 1987). The result is that coronitic rocks at the cores of igneous bodies commonly record near-peak conditions of metamorphism better than their recrystallized margins, as the latter are also more readily retrograde, again due to the presence of fluid that allows the development of hydrous phases at amphibolite-facies conditions. Application of thermobarometry to coronitic rocks is particularly difficult because the presence of coronas suggests global disequilibrium. However, a detailed

(a)



PARAUTOCHTHONOUS BELT

300 km

 MIZ Manicouagan Imbricate Zone

 Paleoproterozoic sedimentary rocks

 Trans Labrador Batholith

MLT Molson Lake terrane

GT Gagnon terrane

 ALLOCHTHONOUS BELT

HJT Hart Jaune terrane

petrographic study may allow identification of domains in which local (domainal) equilibrium can be assumed, and which can be used for determinations of P and T.

Coronitic gabbros in the southern part of the parautochthonous belt of the eastern Grenville Province have been shown to record P–T conditions up to eclogite facies (e.g., Indares 1993, Indares & Rivers 1995). It seems likely, therefore, that coronitic textures have resulted from incomplete transformation at high-pressure and high-temperature (high-P–T) conditions. Evidence for high-P–T conditions is only preserved where fluid infiltration is limited or absent during retrogression and exhumation. The Manicouagan Imbricate Zone, eastern Grenville Province, contains a variety of mafic units with coronitic rocks (e.g., Indares *et al.* 1994). Among them, the Lac Espadon suite (LES) in the Boundary zone consists of lenses of ca. 1650–1630 Ma (Labradorian) coronitic mafic and ultramafic rocks along with amphibolites that were metamorphosed under high-P–T conditions during the Grenvillian Orogeny (ca. 1050–1000 Ma; Cox *et al.* 1998). Our aim in this study is to describe the textures of the mafic and ultramafic rocks of the LES, and to determine the P–T conditions under which they developed.

GEOLOGICAL SETTING

The Manicouagan Imbricate Zone is a 2000 km² stack of high-P crustal rocks exposed along the shores of the Manicouagan Reservoir in eastern Quebec. It occurs at the same structural level as the Molson Lake terrane (Fig. 1a), which has previously been reported to contain eclogitized metagabbro (Rivers *et al.* 1989, Indares & Rivers 1995). To the north, both the Manicouagan Imbricate Zone and the Molson Lake terrane tectonically overlie a Grenvillian fold–thrust and nappe belt (the Gagnon terrane) along a thrust contact. To the south, the Manicouagan Imbricate Zone is overlain by the Hart Jaune terrane along an extensional shear-zone (Fig. 1a). The Hart Jaune terrane experienced medium-P metamorphism during the Grenvillian orogeny.

The Manicouagan Imbricate Zone consists of two fault-bounded lithotectonic packages. The lower package, known as the Lelukuau terrane (Fig. 1b), is a stack of thrust slices largely composed of Labradorian (ca. 1650 Ma) rocks that are considered to represent an igneous AMCG (anorthosite-mangerite-charnockite-granite) suite. The terrane has experienced high-P–T

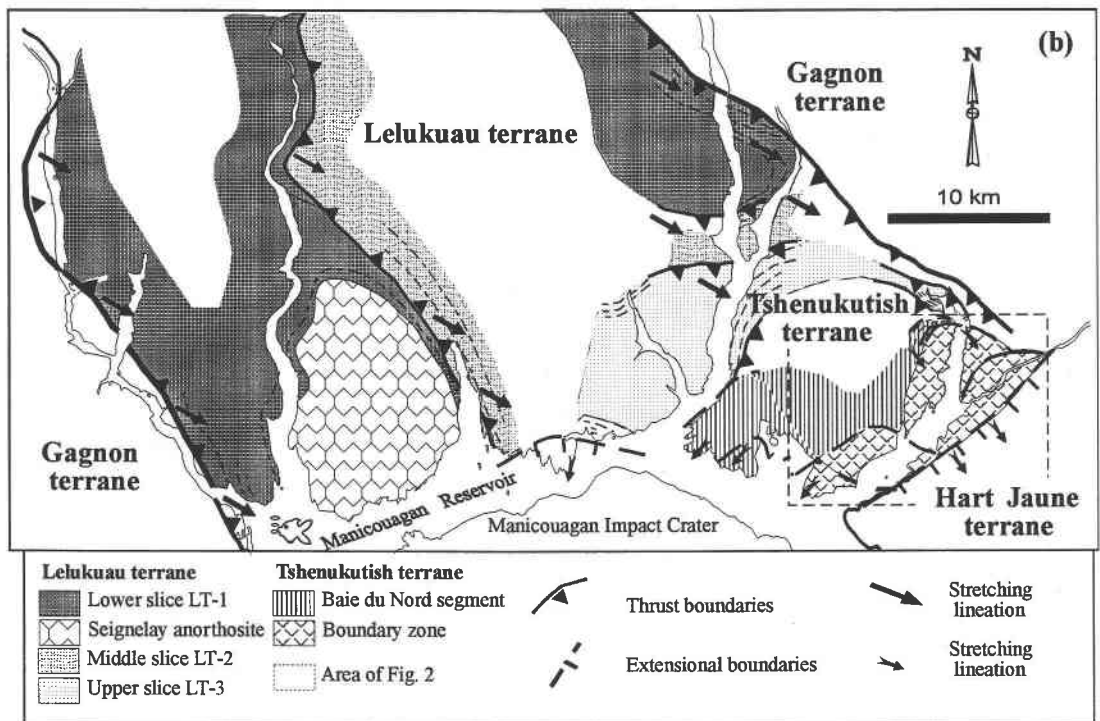


FIG. 1. Maps showing a) location of the Manicouagan Imbricate Zone in the eastern Grenville Province, and b) simplified lithotectonic framework of the Manicouagan Imbricate Zone. Note: the tectonic divisions are from Indares *et al.* (1998).

metamorphism (16–18 kbar and 850–900°C; Indares 1997) which was coeval with the emplacement of mafic dykes between 1050 and 1000 Ma (Gale *et al.* 1994, Indares *et al.* 1998). The tectonically overlying Tshenukutish Terrane (Fig. 1b) comprises two lithotectonic segments, the structurally lower Baie du Nord segment and the overlying Boundary zone. Both units are transected and bounded by extensional shear-zones (Fig. 1b), with evidence for top-to-the-southeast or top-to-the-southwest transport (stage-1 extension: Indares *et al.* 1998).

The Baie du Nord segment is mainly composed of *ca.* 1450 Ma megacrystic diorite intruded by *ca.* 1170 Ma Fe–Ti gabbros. The Fe–Ti gabbros show a transition from coronite (770–810°C and 12–14 kbar) in the southwest to eclogite (720–825°C and 14–17 kbar) in the northeast (Cox & Indares 1999). The Boundary zone (Fig. 2) consists of the Hart Jaune granite (1017 ± 2 Ma), the Brien anorthosite (1169 ± 3 Ma; Scott & Hynes 1994) and subordinate metasedimentary rocks. In addition, the Boundary zone contains Labradorian mafic and ultramafic rocks, referred to as the Lac Espadon suite

(LES). To the south, the Boundary zone is bounded by the Hart Jaune shear zone that separates it from the Hart Jaune terrane and truncates all structural features in the Tshenukutish terrane. The Hart Jaune shear zone displays evidence for top-to-the-southeast transport (stage-2 extension: Indares *et al.* 1998).

The LES can be divided into two parts, exposed along the western and eastern shores of the Hart Jaune Arm, and separated by an extensional shear-zone (Fig. 2). The western part comprises ultramafic rocks (troctolite, dunite and hornblendite) and amphibolite that occur locally as tectonic enclaves in a sheared orthogneiss, and an apatite-rich, Fe–Ti mafic intrusion (nelsonite) to the north (Fig. 2). The eastern part of the LES comprises a massive body of mesocratic olivine gabbro. U–Pb geochronology and geochemical data suggest that the ultramafic rocks and the olivine gabbro represent parts of a *ca.* 1650–1630 Ma (Labradorian) mafic to ultramafic complex similar to the AMCG rocks of the Lelukuau terrane. The nelsonite from the northern part of the LES contains metamorphic zircon that gives an upper intercept also suggesting a Labradorian

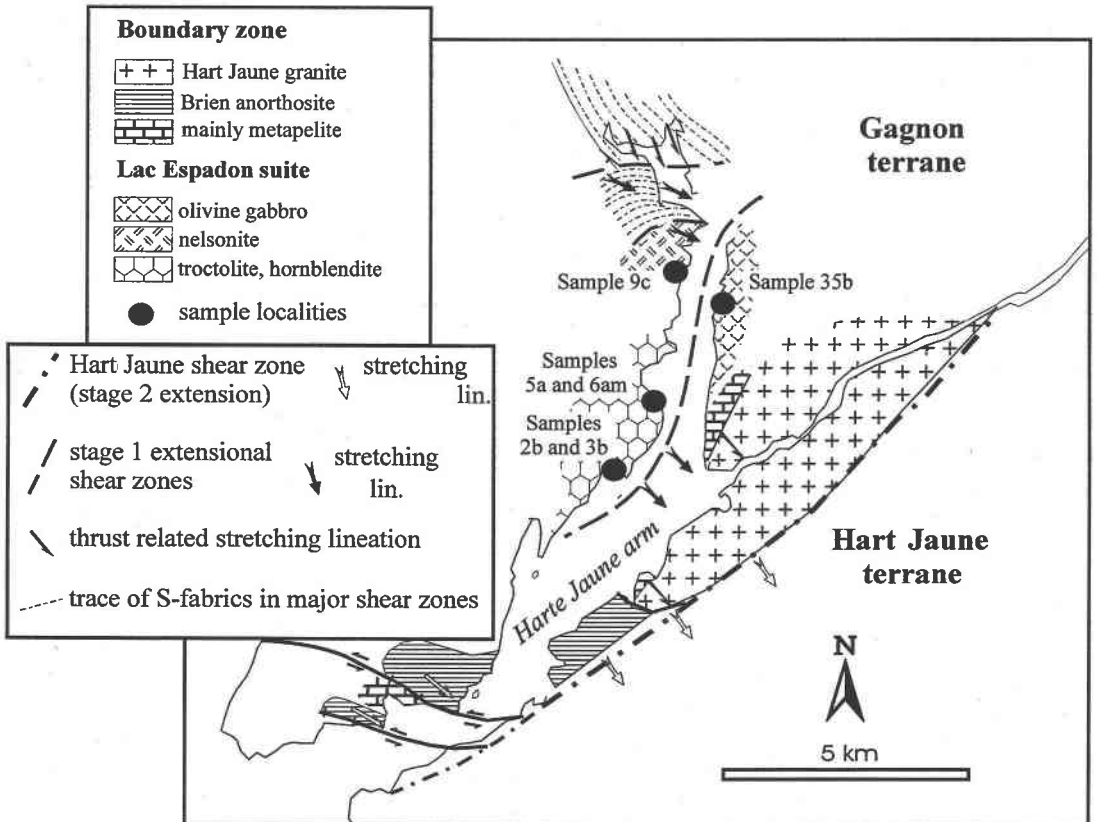


FIG. 2. Map showing the main lithologies, structures and sample localities of the Lac Espadon complex in the Boundary zone.

age of emplacement. U–Pb ages of metamorphic zircon and titanite (*ca.* 1040–1000 Ma) suggest that metamorphism in the LES was contemporaneous with the rest of the Manicouagan Imbricate Zone (Cox *et al.* 1998).

PETROGRAPHY

Sample selection and petrographic study

The samples chosen for detailed petrographic study were collected from the massive parts of the igneous bodies and lenses, and from their deformed margins. The massive parts preserve relics of igneous phases overprinted by high-*P* metamorphic minerals that display textures ranging from coronas to pervasive granoblastic assemblages. The margins comprise foliated granoblastic, amphibole-rich assemblages (amphibolite), indicating extensive infiltration of fluid at some stage of their metamorphic evolution. In order to assess possible differences in metamorphic conditions recorded by the dry interiors and hydrous margins, both were sampled from single outcrops where possible. From the western LES, a troctolite (sample 5a) and its amphibolite margin (sample 6am, olivine garnet amphibolite), a hornblendite (sample 3b) and a garnet amphibolite (sample 2b) were selected along with a sample of nelsonite (sample 9c). From the eastern LES, an olivine gabbro (sample 35b) with granoblastic and coronitic varieties was studied. Sample localities are shown in Figure 2.

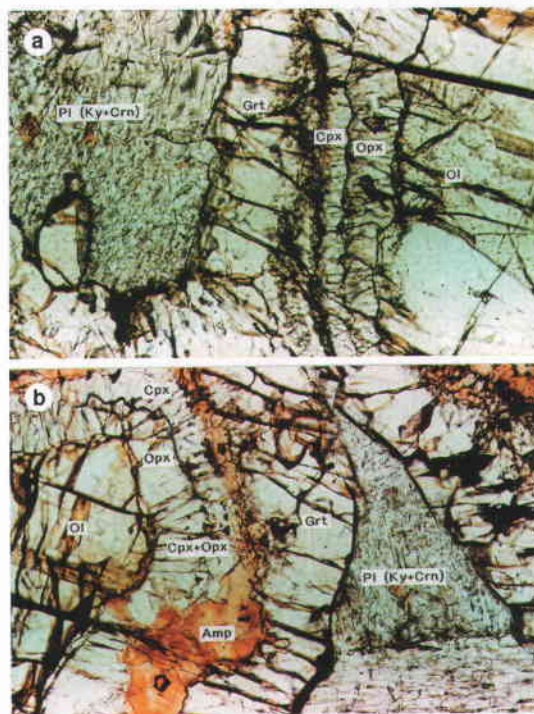
The detailed petrographic study was complemented by cathodoluminescence (CL) microscopy. Sections were examined using a Nuclide Luminoscope unit with doubly magnified objectives, giving magnification from 20× to 640×. Operating conditions varied, but in general an accelerating voltage of 10–15 kV and a beam current of 0.1–2 mA were used. CL images were used to document fine-grained inclusions in relict igneous plagioclase and growth textures of secondary plagioclase in both corona and amphibolite assemblages.

Textures

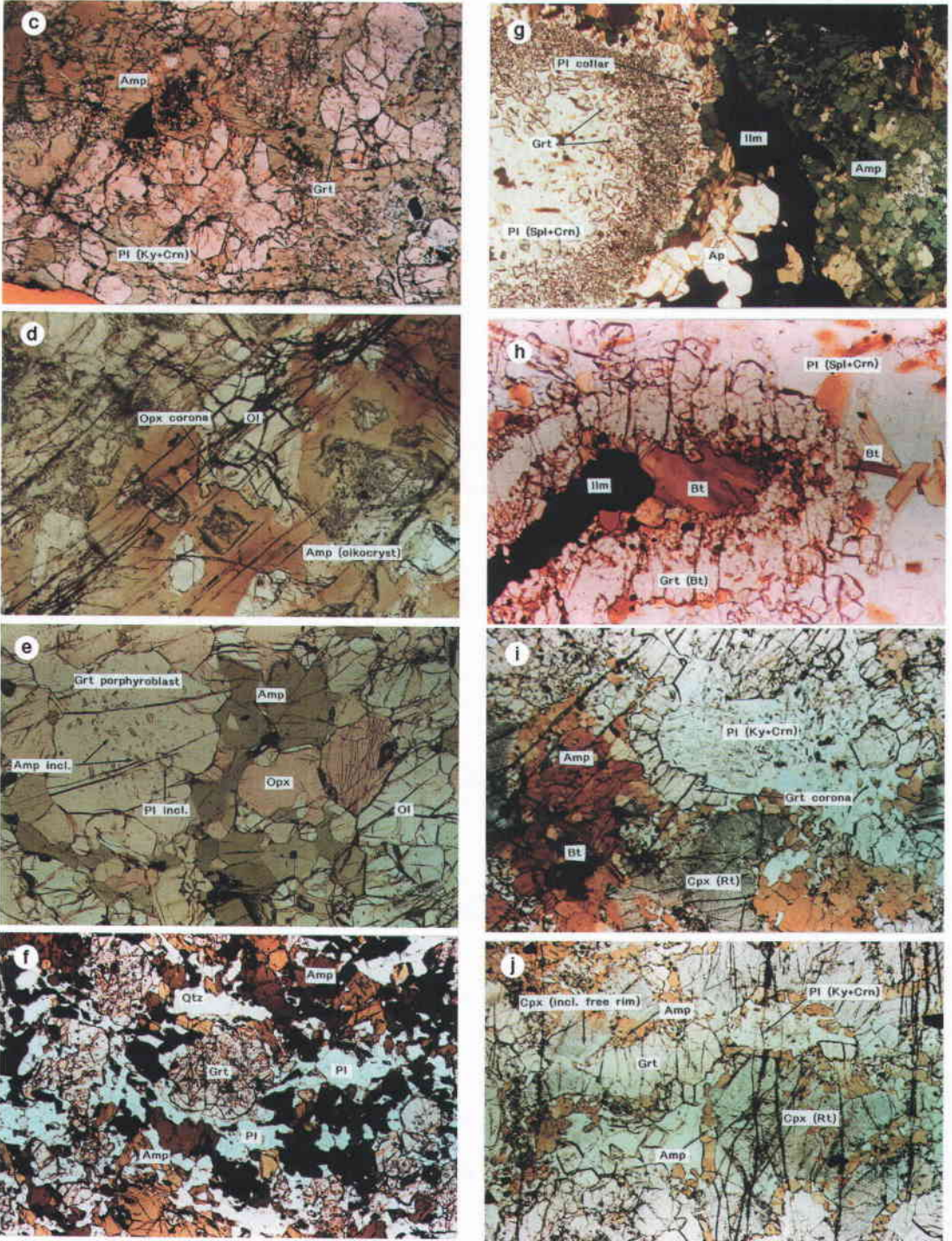
Troctolite (sample 5a): Troctolite and associated rocks from the western LES preserve relict igneous assemblages represented by olivine, plagioclase, and minor ilmenite. Olivine and plagioclase are separated by triple coronas of orthopyroxene, clinopyroxene and garnet (Figs. 3a, b). Grains of plagioclase contain numerous oriented inclusions of kyanite, which shows a bright red CL emission (Fig. 4a), and non-luminescent corundum, which forms small rounded grains. In addition, amphibole and biotite coronas surround ilmenite. Amphibole also occurs locally in the triple coronas growing at the expense of clinopyroxene and garnet. Where amphibole is more extensively developed, clinopyroxene is also partially replaced by orthopyroxene (Fig. 3b). Troctolite grades into coarse-grained dunite containing

minor magnetite and chromite and metamorphic orthoamphibole and serpentine.

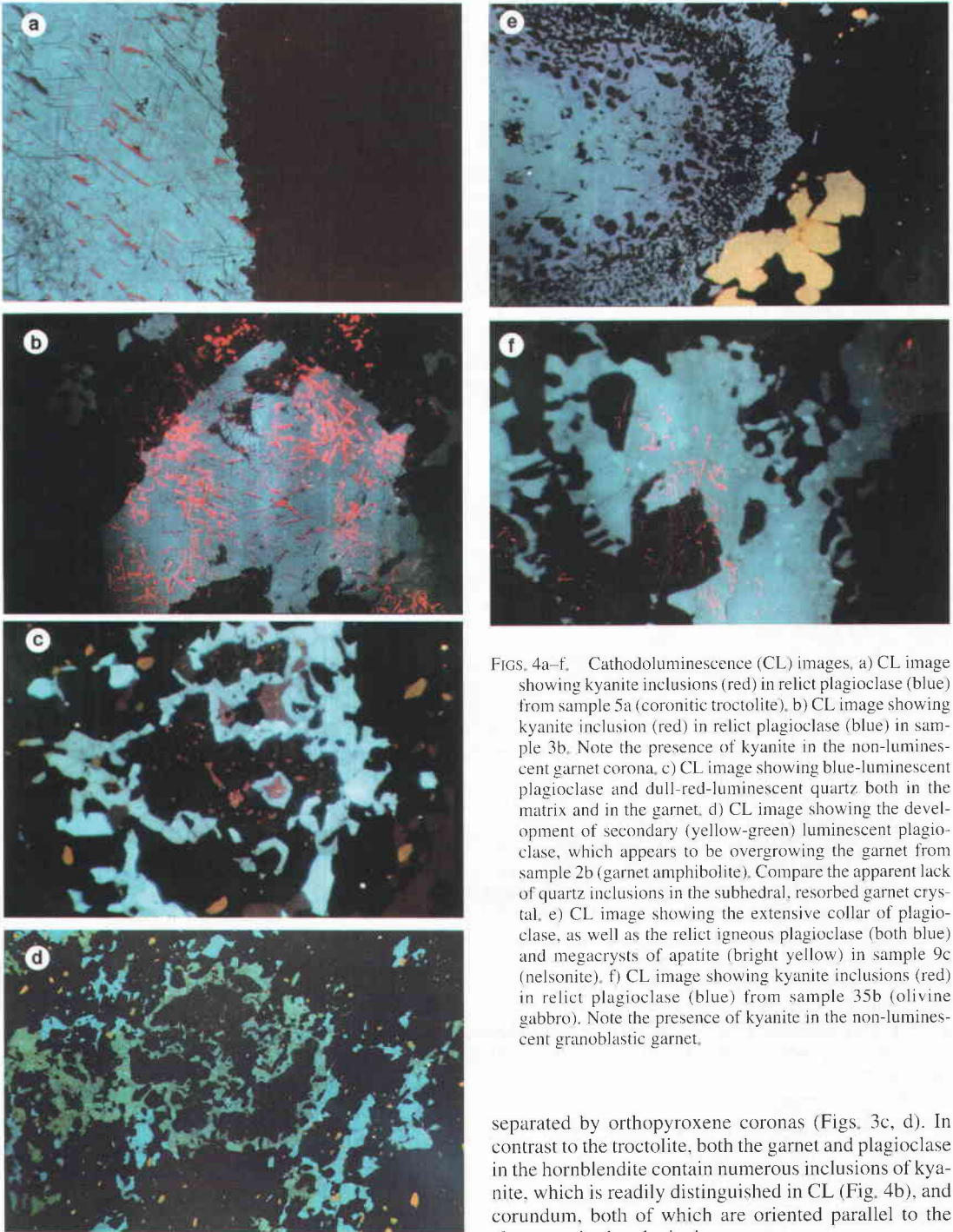
Hornblendite (sample 3b): Small pods of coarse-grained, poikilitic hornblendite are found in close association with dunite and troctolite (Fig. 2). In these rocks, amphibole forms oikocrysts up to 10 cm in diameter. The oikocrysts in association with phlogopite and clinopyroxene megacrysts enclose chadacrysts of olivine, plagioclase and minor proportions of opaque min-



FIGS. 3a–j. Photomicrographs. Troctolite (sample 5a): a) amphibole-free corona assemblage and b) amphibole-bearing corona assemblage. Both images are 0.75 mm wide. Hornblendite (sample 3b): c) general texture with large oikocrysts of amphibole, relict phlogopite and chadacrysts of plagioclase with coronas of garnet, d) clinopyroxene corona around relict olivine chadacryst. Both images are 1.5 mm wide. Olivine garnet amphibolite (Sample 6am): e) garnet porphyroblast and slightly foliated, granoblastic matrix assemblage of amphibole, orthopyroxene and relict olivine. Note the amphibole and plagioclase inclusions in the garnet. Width of image is 1.5 mm. Garnet amphibolite (sample 2b): f) general texture with granoblastic matrix of plagioclase, amphibole and quartz, with minor ilmenite and biotite, and partial resorption of some garnet porphyroblasts. Width of image is 1.5 mm. Nelsonite (sample 9c): g) general texture showing partially preserved corona of garnet adjacent to amphibole, ilmenite and plagioclase, which contains fine-grained spinel and corundum inclusions, h) corona of garnet around ilmenite with abundant biotite inclusions and spinel in plagioclase.



Widths of images are 1.5 and 0.75 mm, respectively. Olivine gabbro (sample 35b): i) garnet corona between plagioclase (which contains numerous inclusions of kyanite and corundum) and ferromagnesian areas, j) granoblastic area with plagioclase, garnet, amphibole and relict clinopyroxene (which contains rutile inclusions). Both images are 1.5 mm wide.



FIGS. 4a–f. Cathodoluminescence (CL) images, a) CL image showing kyanite inclusions (red) in relict plagioclase (blue) from sample 5a (coronitic troctolite), b) CL image showing kyanite inclusion (red) in relict plagioclase (blue) in sample 3b. Note the presence of kyanite in the non-luminescent garnet corona, c) CL image showing blue-luminescent plagioclase and dull-red-luminescent quartz both in the matrix and in the garnet. d) CL image showing the development of secondary (yellow-green) luminescent plagioclase, which appears to be overgrowing the garnet from sample 2b (garnet amphibolite). Compare the apparent lack of quartz inclusions in the subhedral, resorbed garnet crystal, e) CL image showing the extensive collar of plagioclase, as well as the relict igneous plagioclase (both blue) and megacrysts of apatite (bright yellow) in sample 9c (nelsonite), f) CL image showing kyanite inclusions (red) in relict plagioclase (blue) from sample 35b (olivine gabbro). Note the presence of kyanite in the non-luminescent granoblastic garnet.

erals and apatite, and represent the relict igneous assemblage. Plagioclase and amphibole are separated by garnet coronas, whereas olivine and amphibole are

separated by orthopyroxene coronas (Figs. 3c, d). In contrast to the troctolite, both the garnet and plagioclase in the hornblende contain numerous inclusions of kyanite, which is readily distinguished in CL (Fig. 4b), and corundum, both of which are oriented parallel to the cleavages in the plagioclase.

Olivine garnet amphibolite (sample 6am): Deformed margins of troctolite are transformed to granoblastic olivine garnet amphibolite that consists of abundant relict olivine, amphibole and orthopyroxene and is

largely plagioclase-free. The igneous protoliths of these rocks probably contained more olivine and less plagioclase than in the original troctolite. Locally, the olivine garnet amphibolite displays large porphyroblasts of garnet with inclusions of amphibole and small quantities of plagioclase (Fig. 3e). The deformed margins of hornblende, in contrast, do not develop obvious retrograde assemblages. This may be in part due to the hydrous (amphibole-rich) nature of the protolith.

Garnet amphibolite (sample 2b): Granoblastic garnet amphibolite outcrops adjacent to the hornblende (Fig. 2). It is composed of subhedral to anhedral garnet porphyroblasts with equigranular plagioclase, quartz, amphibole and lesser amounts of biotite, rutile, titanite, and ilmenite (Fig. 3f). CL images reveal two generations of plagioclase growth. Plagioclase with a bright blue CL emission appears as inclusions in subhedral porphyroblasts of garnet in association with dull, red-luminescent quartz, and it is also uniformly distributed in the matrix (Fig. 4c). The blue CL emission of the plagioclase is identical to that in the undeformed troctolite and hornblende (and olivine gabbros, see below). However, anhedral porphyroblasts of garnet are rimmed by plagioclase with a yellow CL emission (Fig. 4d). The luminescence colors in plagioclase are caused by small amounts of Ti giving blue and Mn giving yellow CL colors (Marshall 1988). Thus, the breakdown of the Mn-bearing garnet may be responsible for the development of the yellow-luminescent plagioclase in these areas. Titanite also is found in these textural settings growing at the expense of rutile.

Nelsonite (sample 9c): The nelsonite is dominated by large (1–5 cm) crystals of apatite and ilmenite. The original plagioclase has been recrystallized and contains minute inclusions of spinel with rare inclusions of fine-grained corundum (Fig. 3g). Garnet forms irregular coronas between areas rich in mafic phases (ilmenite, amphibole, biotite) and plagioclase. Biotite also occurs as coronas around ilmenite, commonly in association with garnet and also as inclusions in the latter (Fig. 3h). Secondary plagioclase commonly forms between garnet and amphibole, showing up as well-defined blue collars in CL adjacent to the bright yellow apatite. These phases contrast with the non-luminescent garnet, biotite, amphibole and ilmenite (Fig. 4e). Plagioclase collars are interpreted to have grown during decompression (Indares 1993).

Olivine gabbro (sample 35b): In the olivine gabbro from the eastern LES, the original igneous assemblage consists of plagioclase, olivine and clinopyroxene, the latter being rich in rutile inclusions. Large crystals of apatite are common, and minor ilmenite also is present. The olivine gabbro shows more pervasive development of metamorphic textures, ranging from coronitic to granoblastic (Figs. 3i, j). Plagioclase domains preserve an original igneous shape but are extensively recrystallized. Olivine has been replaced by aggregates of orthopyroxene rimmed by coronas of clinopyroxene.

Garnet occurs as discontinuous coronas between clinopyroxene and plagioclase, and locally as granoblastic porphyroblasts. Amphibole is present throughout the olivine gabbros, around original euhedral grains of biotite and ilmenite, and also around clinopyroxene where it is associated with granoblastic garnet and inclusion-poor plagioclase (Fig. 3j). In these areas, relict crystals of clinopyroxene also show a reduction in abundance of rutile inclusions adjacent to the garnet – amphibole – plagioclase contacts. Commonly, both garnet and recrystallized plagioclase cores contain kyanite inclusions, which are evident in CL images (Fig. 4f).

MINERAL CHEMISTRY

Mineral analysis

Garnet, olivine, orthopyroxene, clinopyroxene, amphibole, plagioclase and spinel were analyzed with a CAMECA SX-50 electron microprobe, using a LINK energy-dispersion spectroscopy (EDS) X-ray analyzer. Back-scattered electron (BSE) images were used to examine fine-scale features prior to analysis. The EDS analyzer was calibrated using a Costandard and compared with several mineral standards before and after each run. Conditions for analysis were set at 15 kV accelerating voltage, a beam current of 20 nA and a beam diameter of 1 μm , except for plagioclase which was analyzed using a 10 nA current and a beam diameter of 3 μm to avoid Na loss during analysis. Count times varied from 50 seconds for garnet to 100 seconds for pyroxene and amphibole. Results were corrected using the ZAF software. Typically 50–100 analyses of each mineral in each section were done, along with zoning profiles where appropriate. Representative results of electron-microprobe analyses of mineral compositions are shown in Table 1. The structural formulae for garnet, orthopyroxene, clinopyroxene, amphibole and plagioclase were calculated using THEBA v. 6.0 (J. Martignole *et al.*, unpublished). The Fe^{3+} content of the ferromagnesian minerals was estimated using the method of Droop (1986). All mineral abbreviations are from Kretz (1983) and Spear (1993).

Garnet compositions and zoning

Representative compositions of the garnet are shown in Figure 5. Garnet compositions from the most Mg-rich rocks, *i.e.*, troctolite (in contact with clinopyroxene), hornblende, olivine gabbro and also the olivine garnet amphibolite all have high Mg contents ($>\text{Prp}_{50}$). In contrast, the nelsonite and garnet amphibolite are more Fe-rich, and the garnet has a correspondingly lower Mg contents (*ca.* Prp_{20-30}). Thus there is a correlation between the Mg content in garnet and the bulk-rock composition. On the other hand, the troctolite, hornblende and olivine gabbro contain mineral assemblages indicative of high-P metamorphism, whereas the garnet am-

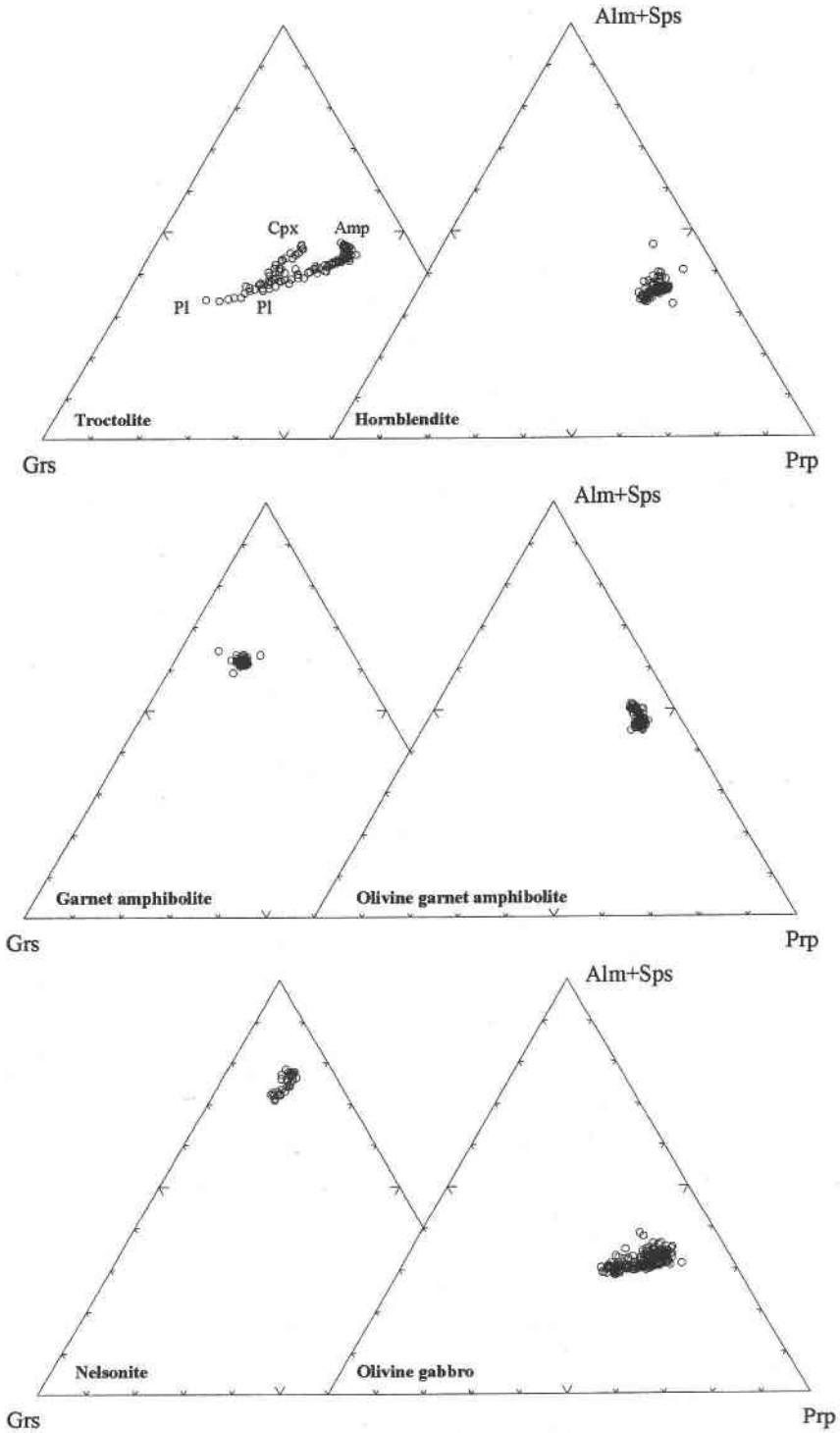


FIG. 5. Garnet compositions plotted as Grs, Alm+Sps and Prp for selected samples from the Lac Espadon suite.

TABLE 1. REPRESENTATIVE COMPOSITIONS OF GARNET, LAC ESPADON SUITE

Sample	5a						6am		3b		35b			2b		9c	
	corona		retrograde				rim	core	corona		corona		rim	cores	rim	corona	
	Cpx	Pl	Amp	Cpx	Opx	Pl			Pl	Amp	Pl	Cpx				Amp	Pl
SiO ₂ wt%	40.02	39.65	40.22	39.25	40.24	39.71	39.69	40.75	41.16	40.75	40.96	41.33	41.03	41.39	38.08	37.71	37.75
Al ₂ O ₃	22.76	22.07	22.74	22.57	22.67	22.51	21.85	22.43	23.38	22.79	23.41	22.99	22.94	23.05	20.62	21.17	21.11
TiO ₂	0.00	0.04	0.09	0.00	0.03	0.00	0.00	0.02	0.10	0.00	0.00	0.00	0.00	0.02	0.00	0.05	0.09
FeO(total)	20.90	20.90	19.78	22.13	20.98	21.38	24.57	23.12	18.63	19.57	15.94	16.34	16.24	14.96	26.57	33.90	33.85
MgO	11.01	7.61	10.38	10.74	11.02	8.17	10.77	11.94	13.31	12.38	12.06	13.42	14.33	12.01	2.89	3.52	3.56
MnO	0.50	0.50	0.39	0.53	0.44	0.37	0.90	0.52	0.43	0.74	0.37	0.40	0.43	0.26	2.42	1.79	1.89
CaO	5.87	10.25	7.92	5.82	6.43	9.57	3.09	3.34	5.78	5.63	9.12	7.25	5.79	10.56	10.79	4.08	4.23
Total	101.09	101.06	101.56	101.11	101.87	101.76	100.95	102.12	102.82	101.92	101.88	101.78	100.79	102.30	101.54	102.32	102.60
Si <i>apfu</i>	2.98	3.00	2.99	2.95	2.98	2.98	3.00	3.01	2.98	3.00	2.98	3.00	3.00	2.99	2.99	2.97	2.97
Al	2.00	1.97	1.96	2.00	1.98	1.99	1.95	1.95	2.00	1.97	2.01	1.97	1.98	1.96	1.91	1.96	1.96
Ti	0.00	0.01	0.04	0.00	0.00	0.00	0.00	0.00	0.05	0.00	0.00	0.00	0.00	0.00	0.00	0.00	0.00
Fe ²⁺	1.29	1.29	1.16	1.34	1.27	1.32	1.50	1.38	1.11	1.17	0.97	0.95	0.97	0.85	1.65	2.17	2.17
Fe ³⁺	0.01	0.03	0.05	0.05	0.03	0.03	0.05	0.04	0.02	0.03	0.01	0.03	0.02	0.04	0.10	0.06	0.06
Mg	1.22	0.86	1.09	1.20	1.22	0.91	1.21	1.32	1.44	1.36	1.31	1.53	1.56	1.28	0.34	0.41	0.42
Ca	0.47	0.83	0.75	0.47	0.51	0.77	0.25	0.26	0.50	0.44	0.71	0.50	0.45	0.86	0.91	0.34	0.35
Mn	0.03	0.03	0.03	0.03	0.03	0.02	0.06	0.03	0.03	0.05	0.02	0.02	0.03	0.03	0.16	0.12	0.11
Total	8.01	8.01	8.03	8.05	8.02	8.02	8.02	7.99	8.02	8.02	8.01	8.01	8.01	8.02	8.05	8.05	8.04
X _{Alm}	0.428	0.429	0.401	0.440	0.419	0.435	0.497	0.462	0.367	0.388	0.321	0.320	0.322	0.292	0.530	0.712	0.705
X _{Prp}	0.406	0.285	0.381	0.395	0.403	0.302	0.402	0.439	0.476	0.449	0.435	0.484	0.519	0.431	0.128	0.136	0.137
X _{Grs}	0.149	0.260	0.197	0.130	0.151	0.241	0.057	0.065	0.136	0.132	0.234	0.173	0.139	0.257	0.230	0.081	0.078
X _{Spn}	0.010	0.011	0.008	0.011	0.009	0.008	0.019	0.011	0.009	0.015	0.008	0.008	0.009	0.005	0.051	0.039	0.041

Number of ions expressed in atoms per formula unit (*apfu*). Nature of the samples: 5a troctolite, 6am olivine garnet amphibolite, 3b hornblende, 35b olivine gabbro, 2b garnet amphibolite, 9c nelsonite. The last line of column headings indicates the mineral with which the garnet is in contact.

phibolite has amphibolite-facies assemblages. The olivine garnet amphibolite contains evidence for both high-P metamorphism, *e.g.*, coexisting garnet and olivine (Harley & Carswell 1990) and re-equilibration, *e.g.*, orthopyroxene and amphibole. Thus there may also be a correlation between the type of mineral assemblage (high-P *versus* retrograde) and whole-rock chemical composition.

Garnet zoning profiles are shown in Figures 6a–h. The garnet coronas in the troctolite (sample 5a) are strongly zoned. In amphibole-free coronas, Ca increases toward the plagioclase, with a maximum Grs₄₈ adjacent to the contact. This is compensated by decreasing Fe and Mg from clinopyroxene (Prp₃₉Alm₄₂) to plagioclase (Prp₁₉Alm₃₂) contacts (Fig. 6a). The X_{Fe} [(*i.e.*, Fe/(Fe+Mg))] in these garnet coronas increases in conjunction with Ca content. The above patterns are typical of growth zoning in coronitic garnet (Indares & Rivers 1995, Indares & Dunning 1997). Since coronitic garnet grows from the inner to outer rim between reactant

phases instead of concentrically outward, zoning is controlled by the chemical gradient between the minerals at the growth interfaces. In other words, the garnet corona has higher Ca toward the plagioclase and higher Fe and Mg toward the clinopyroxene. In the coronas where orthopyroxene and amphibole replace clinopyroxene, garnet zoning displays a similar trend, but in addition there is a reversal at the garnet rims. In such cases, the Ca content drops from a maximum of Grs₄₀ to Grs₃₅ at the garnet–plagioclase contact. Mg decreases to Prp₃₇, and Fe increases to Alm₄₅ (Fig. 6b) at the clinopyroxene–orthopyroxene–pargasite (triple-junction) contact. The reversal in zoning is interpreted to be the result of retrograde resetting. The amphibole-bearing garnet coronas also show less strong X_{Fe} zonation, probably due to the effects of chemical re-equilibration.

Garnet coronas in the hornblende (sample 3b) are weakly zoned (Fig. 6c), with compositions ranging from Alm₃₉Prp₄₅Grs₁₃ (amphibole contact) to Alm₃₅Prp₄₉Grs₁₃ (plagioclase contact), probably due to homogeni-

TABLE 1 (continued). REPRESENTATIVE COMPOSITIONS OF PLAGIOCLASE, LAC ESPADON SUITE

Sample	5a		6am	3b	35b		2b	9c
	relict	relict (retrograde)	incl.	relict	relict	relict (retrograde)	matrix	relict
SiO ₂ wt%	58.29	60.05	64.39	60.21	59.87	59.98	60.27	64.20
Al ₂ O ₃	26.65	24.63	23.18	25.89	25.13	25.49	24.93	23.24
FeO (total)	0.24	0.69	0.31	0.17	0.12	0.12	0.43	0.19
CaO	7.72	6.16	4.13	6.62	6.83	7.15	6.68	4.24
Na ₂ O	7.35	7.60	8.88	7.03	7.76	7.58	7.75	8.72
K ₂ O	0.26	0.20	0.12	0.03	0.24	0.19	0.26	0.12
Total	100.51	99.33	101.01	99.95	99.95	100.5	100.32	100.71
Si <i>apfu</i>	2.69	2.66	2.81	2.66	2.67	2.66	2.68	2.81
Al	1.30	1.33	1.19	1.37	1.32	1.33	1.31	1.20
Fe ²⁺	0.03	0.01	0.01	0.01	0.00	0.00	0.02	0.01
Ca	0.30	0.33	0.19	0.32	0.33	0.34	0.32	0.20
Na	0.66	0.67	0.75	0.61	0.67	0.65	0.67	0.74
K	0.01	0.02	0.01	0.00	0.01	0.01	0.01	0.01
Total	4.99	5.02	4.97	4.96	5.01	5.00	5.01	4.96
X _{An}	0.362	0.306	0.210	0.342	0.323	0.339	0.318	0.210
X _{Ab}	0.624	0.683	0.790	0.656	0.664	0.650	0.668	0.783
X _{Or}	0.015	0.012	0.000	0.002	0.014	0.011	0.015	0.007

Nature of the samples: 5a troctolite, 6am olivine garnet amphibolite, 3b hornblende, 35b olivine gabbro, 2b garnet amphibolite, 9c nelsonite.

TABLE 1 (continued). REPRESENTATIVE COMPOSITIONS OF AMPHIBOLE, LAC ESPADON SUITE

Sample	5a	6am	3b	35b	2b	9c
	retro	matrix	oikocryst	retro	matrix	corona
SiO ₂ wt%	42.49	40.31	44.15	43.49	43.08	42.31
Al ₂ O ₃	15.57	12.33	15.46	15.78	12.79	12.94
TiO ₂	0.93	1.76	0.11	0.63	0.50	0.60
FeO (total)	6.70	18.45	15.95	5.53	18.46	19.03
MnO	0.07	0.16	0.00	0.03	0.21	0.08
MgO	15.34	8.64	11.65	15.90	9.72	9.52
NiO	0.09	0.08	0.47	0.15	0.00	0.00
CaO	11.91	11.63	3.36	12.34	10.84	10.48
Na ₂ O	2.88	1.89	6.01	2.30	1.75	1.83
K ₂ O	1.10	1.81	0.01	1.12	0.53	0.67
Total	97.19	97.10	97.29	97.52	97.89	97.53
Si <i>apfu</i>	6.15	6.22	6.28	6.22	6.46	6.40
Al	2.66	2.24	2.59	2.66	2.63	2.31
Ti	0.10	0.20	0.01	0.07	0.06	0.07
Fe ²⁺	0.69	2.24	0.60	0.56	1.72	1.72
Fe ³⁺	0.12	0.14	0.25	0.10	0.60	0.69
Mn	0.01	0.02	0.00	0.00	0.03	0.01
Mg	3.31	1.99	3.38	3.39	2.17	2.15
Ni	0.01	0.01	0.05	0.02	0.00	0.00
Ca	1.85	1.92	1.78	1.89	1.74	1.70
Na	0.81	0.56	0.93	0.64	0.51	0.54
K	0.20	0.36	0.00	0.20	0.10	0.13
Total	15.92	15.92	15.96	15.79	16.02	15.71

Nature of the samples: 5a troctolite, 6am olivine garnet amphibolite, 3b hornblende, 35b olivine gabbro, 2b garnet amphibolite, 9c nelsonite.

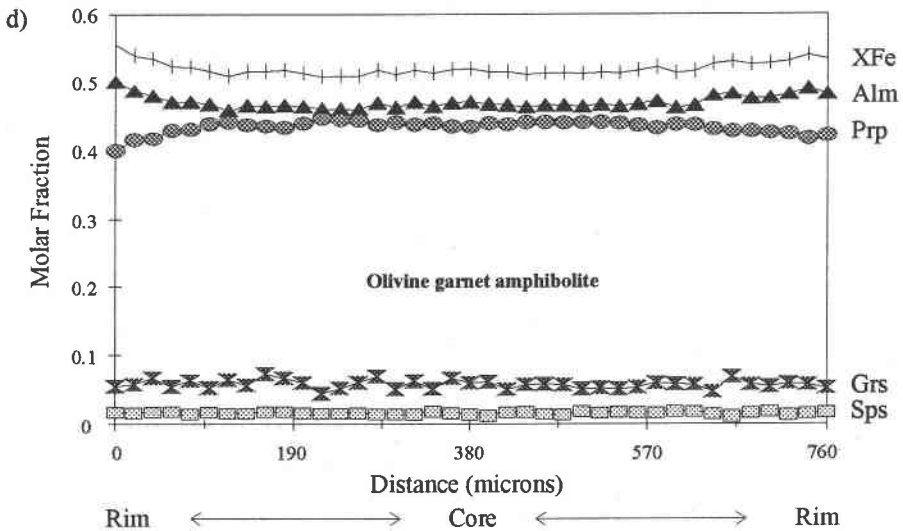
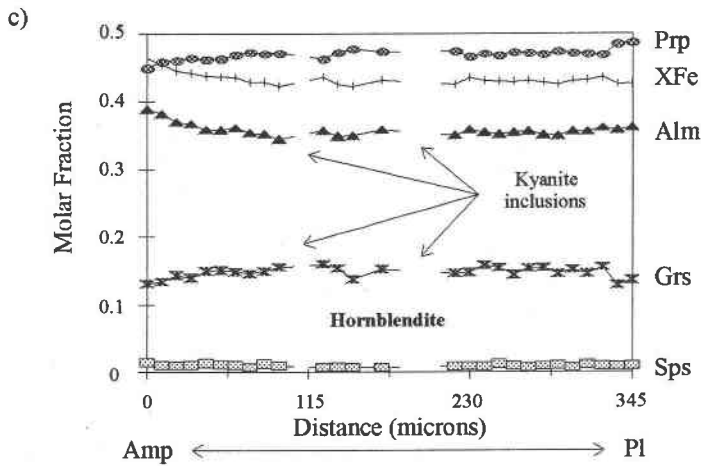
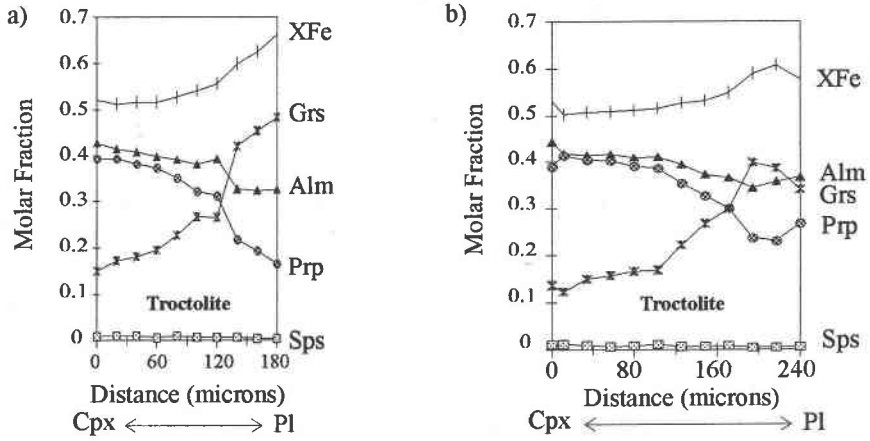
TABLE 1 (continued). REPRESENTATIVE COMPOSITIONS OF CLINOPYROXENE, ORTHOPYROXENE, OLIVINE AND SPINEL, LAC ESPADON SUITE

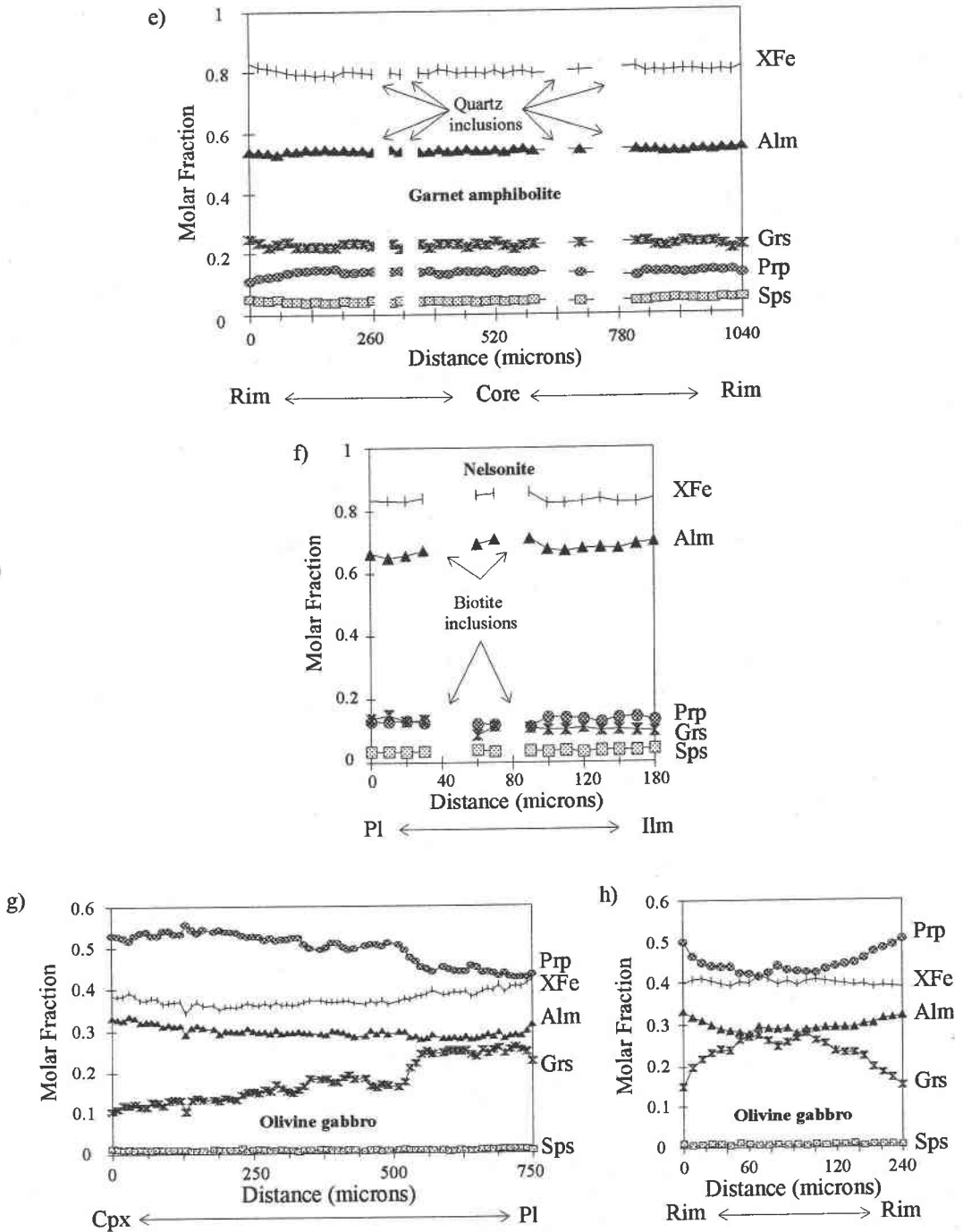
Sample	5a		35b		5a	6am	9c		
	Cpx corona	Cpx incl. Grt-con	Cpx corona	Cpx corona grano. Grt-con	Opx corona	Opx matrix	Ol matrix incl.		
SiO ₂ wt%	54.06	53.75	54.23	53.22	53.39	54.53	53.29	37.22	0.77
Al ₂ O ₃	3.92	4.76	3.00	5.06	5.18	1.77	2.59	0.00	60.48
TiO ₂	0.18	0.27	0.09	0.27	0.18	0.03	0.09	0.00	0.00
FeO (total)	5.13	5.22	4.66	3.31	3.64	15.81	18.14	30.12	27.10
MgO	14.21	13.69	15.21	14.78	14.59	27.52	25.53	32.51	9.21
MnO	0.07	0.02	0.12	0.09	0.00	0.11	0.20	0.33	0.08
Cr ₂ O ₃	0.17	0.00	0.27	0.16	0.34				0.00
NiO	0.12	0.04	0.00	0.00	0.13				0.14
ZnO									1.37
CaO	21.31	21.45	22.60	23.23	22.85	0.23	0.07	0.07	
Na ₂ O	1.53	1.59	0.97	1.06	1.32				
Total	100.72	100.80	101.20	101.23	101.74	100.00	99.91	100.25	99.15
Si <i>apfu</i>	1.96	1.95	1.96	1.91	1.91	1.96	1.94	1.00	0.021
Al	0.17	0.20	0.13	0.21	0.22	0.08	0.11	0.00	1.933
Ti	0.01	0.01	0.00	0.01	0.01	0.00	0.01	0.00	0.000
Fe ²⁺	0.15	0.16	0.13	0.08	0.07	0.47	0.55	0.68	0.621
Fe ³⁺	0.01	0.00	0.01	0.02	0.04	0.00	0.01	0.00	0.000
Mg	0.77	0.74	0.82	0.79	0.78	1.47	1.38	1.31	0.376
Mn	0.00	0.00	0.00	0.00	0.00	0.00	0.01	0.02	0.002
Cr	0.01	0.00	0.02	0.01	0.01				0.000
Ni	0.02	0.01	0.00	0.00	0.01				0.003
Zn									0.028
Ca	0.83	0.83	0.87	0.89	0.88	0.02	0.00	0.00	
Na	0.11	0.11	0.07	0.07	0.09				
Total	4.00	4.00	4.00	4.01	4.01	4.00	4.00	3.00	2.983
X _{Fs}	0.161	0.175	0.135	0.095	0.087				
X _{Fs}	0.839	0.825	0.865	0.905	0.913				
X _{Ab}	0.008	0.001	0.013	0.017	0.035				
X _{Sp}	0.100	0.111	0.055	0.057	0.057				

Nature of the samples: 5a troctolite, 6am olivine garnet amphibolite, 35b olivine gabbro, 9c nelsonite.

zation at elevated temperatures. XFe also increases with Fe content. Large porphyroblasts of garnet from the garnet olivine amphibolite (sample 6am) show a weak increase in Fe content and decrease in Mg content (Fig. 6d) from the core (Alm₄₅Prp₅₀) to the rim (Alm₅₀Prp₄₇), along with an increase in XFe. These porphyroblasts are unzoned with respect to Ca, and indeed Grs contents are low (Grs₀₅). The lack of zoning displayed in the core of the garnet porphyroblasts suggests high-T homogenization. The increase in XFe toward the rim (Fig. 6d) indicates that Fe–Mg exchange continued between garnet rims and adjacent phases during cooling.

Both subhedral and resorbed garnet porphyroblasts in the garnet amphibolite (sample 2b) are homogeneous. The subhedral grains (Fig. 6e) locally display a slight decrease in Mg (Prp_{45–40}) and increase in Fe and Mn toward the rims (Alm_{45–50}Sps_{02–05}), along with an increase in XFe. The increase in XFe toward the garnet rim suggests retrograde resetting. Garnet coronas from the nelsonite (sample 9c) also are weakly zoned (Fig.





FIGS. 6a-h. Garnet zoning profiles for a) sample 5a (coronitic troctolite), amphibole-free corona, c) sample 3b (hornblende), kyanite-bearing garnet corona around a plagioclase chadacryst, d) sample 6am (olivine amphibolite), zoning traverse across a garnet porphyroblast, e) sample 2b (garnet amphibolite), traverse across a subhedral porphyroblast, f) sample 9c (nelsonite), garnet corona with biotite inclusions, g) sample 35b (olivine gabbro), large garnet corona around a relict igneous clinopyroxene, and h) small kyanite-bearing garnet. Symbols on all profiles: square: spessartine, cross: grossular, circle: pyrope, triangle: almandine and dash: Fe/(Fe + Mg).

6f), with Ca increasing slightly and Fe decreasing toward the plagioclase (Alm₇₀Grs₁₀ to Alm₆₅Grs₁₅). XFe increases toward biotite inclusions in the corona. In addition, the garnet compositions are higher in Mn content (Sps₀₃) than in the other samples. Thus, the garnet zoning profiles in the nelsonite show clear evidence of homogenization and retrograde Fe–Mg exchange with biotite inclusions.

The olivine gabbro from the eastern LES (sample 35b) displays areas with both coronitic and porphyroblastic garnets. In coronitic examples, garnet compositions generally increase in Ca (Grs_{27–10}) and decrease in Mg (Prp_{48–52}) toward the plagioclase contacts (Fig. 6g). XFe also increases along with Ca. Garnet porphyroblasts (Fig. 6h) also are zoned, with (kyanite-bearing) cores richer in Ca (Alm₂₈Prp₄₂Grs₂₇) and rims richer in Fe and Mg (Alm₃₂Prp₅₀Grs₁₅). This finding indicates that despite their granoblastic texture, these garnet porphyroblasts may have replaced original plagioclase domains,

and the zoning may be a relict growth-related feature. However, the XFe content of the garnet porphyroblasts is homogeneous, presumably because the garnet porphyroblasts were partially homogenized during high-T metamorphism.

Clinopyroxene, plagioclase and amphibole compositions

In contrast to the garnet, clinopyroxene, plagioclase and amphibole display more restricted compositional ranges. The clinopyroxene compositions from the both the troctolite and olivine gabbro (Fig. 7) are all sodian augite, (Di + Hd)_{80–95}(Jd + Ae)_{5–20}.

Plagioclase compositions for the troctolite and hornblende lie in the range An_{40–30}Ab_{60–70} (Fig. 8). Plagioclase from the garnet amphibolite (sample 2b) and plagioclase inclusions in garnet poikiloblasts from the olivine garnet amphibolite (sample 6am) are slightly

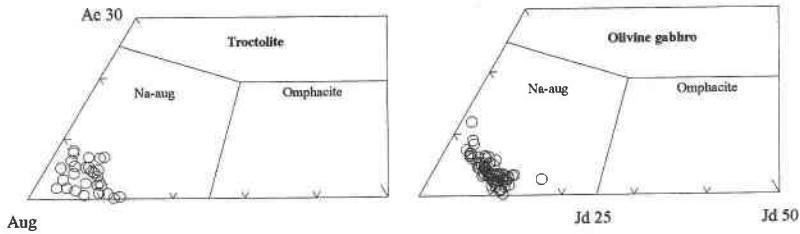


FIG. 7. Compositional diagrams for clinopyroxene for the troctolite and olivine gabbro in the Lac Espadon suite.

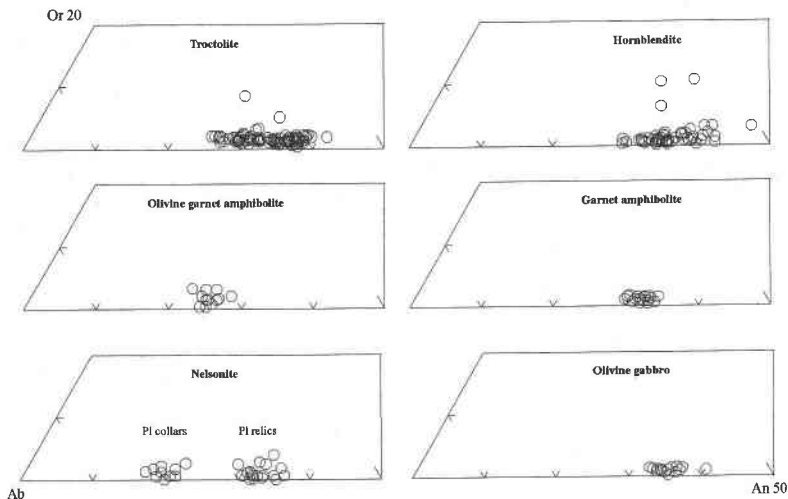


FIG. 8. Plagioclase compositions for samples in the Lac Espadon suite.

more sodic (An₃₂₋₂₂Ab₆₈₋₇₈). Plagioclase compositions in the olivine gabbro lie in the range An₃₂₋₃₀Ab₆₈₋₆₀. In the nelsonite, the plagioclase with spinel inclusions ranges in composition from An₃₈Ab₆₂ to An₃₀Ab₇₀, whereas the secondary collars are more sodic (An₂₅₋₁₈Ab₇₅₋₈₂).

In all samples, the amphiboles lie in the compositional range pargasite – ferropargasite – ferroedenite (Fig. 9). Samples with the best-preserved textural evidence for high-P metamorphism (troctolite, hornblende and olivine gabbro) also contain the most magnesian compositions of pargasite. This finding is consistent with the interpretation that the pargasitic amphibole grew as a replacement of high-P (Mg-rich) garnet and clinopyroxene in the presence of fluid shortly after peak conditions. The amphibole-rich rocks, olivine garnet amphibolite, garnet amphibolite and nelsonite, contain the most Fe-rich pargasitic amphiboles. Amphibole compositions in the olivine garnet amphibolite are the most Na-rich, lying close to the pargasite–edenite compositional boundary (Fig. 9). The more Fe-rich compositions in these samples may be the result of re-equilibration with garnet or other Fe-rich phases during retrogression.

INTERPRETATION OF TEXTURES AND THERMOBAROMETRY

General approach

For each sample, the interpretation of textures and of mineral compositions was followed by selection of appropriate microdomains for P–T determinations. These are domains in each sample for which local equilibrium may be inferred, and pressure- and temperature-dependent reactions can be written. Temperatures were calculated using garnet–clinopyroxene, garnet–orthopyroxene, garnet–olivine and garnet–amphibole Fe–Mg exchange reactions. Pressures were calculated using the garnet – plagioclase – kyanite – corundum reaction (Indares & Rivers 1995) for the troctolite, hornblende and olivine gabbro. The assemblage garnet – plagioclase – quartz – rutile – titanite was used as a variation of the GRAIL barometer (*e.g.*, Ghent & Stout 1984) in the garnet amphibolite. The garnet – plagioclase – spinel – corundum reaction after Indares & Dunning (1997) was used for estimates of P in the nelsonite. Owing to the lack of contacts between granoblastic domains and plagioclase inclusions in the olivine garnet amphibolite, independent pressures could not be calculated for this sample. Given the errors associated with the estimation of the Fe³⁺ content, all temperatures were calculated assuming the Fe to be Fe²⁺.

Temperatures and pressures were calculated using appropriate reactions with the program TWEEQU v. 2.02 (Berman 1991) that uses an internally consistent database. Activity models used are those of Fuhrman & Lindsley (1988) for plagioclase, and Berman *et al.* (1995) and Berman & Aranovich (1996) for olivine,

pyroxene and garnet. For garnet–amphibole thermometry, version 1.01 of the program was used (Berman, pers. commun.) with the activity model of Mäder & Berman (1992) for amphibole and Berman (1990) for garnet. The results were compared with the Fe–Mg exchange thermometers of Ellis & Green (1979) and Krogh (1988) for garnet–clinopyroxene, Carswell & Harley (1990) for garnet–orthopyroxene, O'Neill & Wood (1980) for garnet–olivine, and Graham & Powell (1984) for garnet–amphibole because these have been extensively used in the literature. The P–T conditions

TABLE 2. CONDITIONS OF PRESSURE AND TEMPERATURE RECORDED BY THE MAFIC SAMPLES OF THE LAC ESPADON SUITE

Thermometry (T range in pressure interval from 0 to 20 kbar)						
	TWEEQU	E&G79	K88	C&H90	O&W80	G&P84
1	780–870	720–810	670–765			
2	700–775	650–715	600–660			
3	790–890	730–830	695–790			
4	685–790			750–865		
5	745–810					760–825
6	650–860				710–915	
7	590–670				685–730	
8	605–700			665–815		
9	610–720					640–750
10	800–925					825–950
11	620–795					630–705
12	550–690					485–560
13	750–860	760–880	715–825			765–880
14	775–870	790–885	745–840			

Barometry (all TWEEQU; P range for temperature interval shown above)			
	Grt–Pl–Ky–Crn	GRAIL+Ttn	Grt–Pl–Spl–Crn
1	15.5–18.5		
2	13.5–15.75		
3	14.5–17		
10	14.75–19		
11		9.75–11.75	
12			4–5.5
13	12–14		
14	14.5–16.25		

List of rock types and assemblages: 1 Sample 5a, coronitic troctolite, Amp-free corona assemblage Grt–Cpx–Pl–Ky–Crn (contacts). 2 Sample 5a, coronitic troctolite, Amp-bearing corona assemblage, Grt–Cpx–Pl–Ky–Crn (contacts). 3 Sample 5a, coronitic troctolite, Amp-bearing corona assemblage, Grt–Cpx (incl.). 4 Sample 5a, coronitic troctolite, Amp-bearing corona assemblage, Grt–Opx (contacts). 5 Sample 5a, coronitic troctolite, Amp-bearing corona assemblage, Grt–Amp (contacts). 6 Sample 6am, olivine garnet amphibolite, garnet porphyroblast core and rim, Grt–Ol (cores). 7 Sample 6am, olivine garnet amphibolite, garnet porphyroblast core and rim, Grt–Ol (contacts). 8 Sample 6am, olivine garnet amphibolite, garnet porphyroblast core and rim, Grt–Opx (contacts). 9 Sample 6am, olivine garnet amphibolite, garnet porphyroblast core and rim, Grt–Amp (contacts). 10 Sample 3b, hornblende, corona assemblage, Grt–Amp–Pl–Ky–Crn (contacts). 11 Sample 2b, garnet amphibolite, Grt rims and matrix, Grt–Amp–Pl–Qtz–Ttn–Rt (contacts). 12 Sample 9c, nelsonite, corona assemblage, Grt–Amp–Pl–Spl–Crn (contacts). 13 Sample 35b, olivine gabbro, granoblastic assemblage, Grt–Cpx–Pl–Ky–Crn (rims). 14 Sample 35b, olivine gabbro, granoblastic assemblage, Grt–Cpx–Pl–Ky–Crn (contacts). Abbreviations for the conventional thermometers: E&G79: Ellis & Green (1979), K88: Krogh (1988) for garnet–clinopyroxene, C&H90: Carswell & Harley (1990) for garnet–orthopyroxene, O&W80: O'Neill & Wood (1980) for garnet–olivine, G&P84: Graham & Powell (1984) for garnet–amphibole. Barometric reactions are taken from Indares & Rivers (1995) for garnet – plagioclase – kyanite – corundum, Ghent & Stout (1984) for garnet – plagioclase – rutile – quartz – titanite (GRAIL + Ttn variant), and Indares & Dunning (1997) for garnet – plagioclase – spinel – corundum.

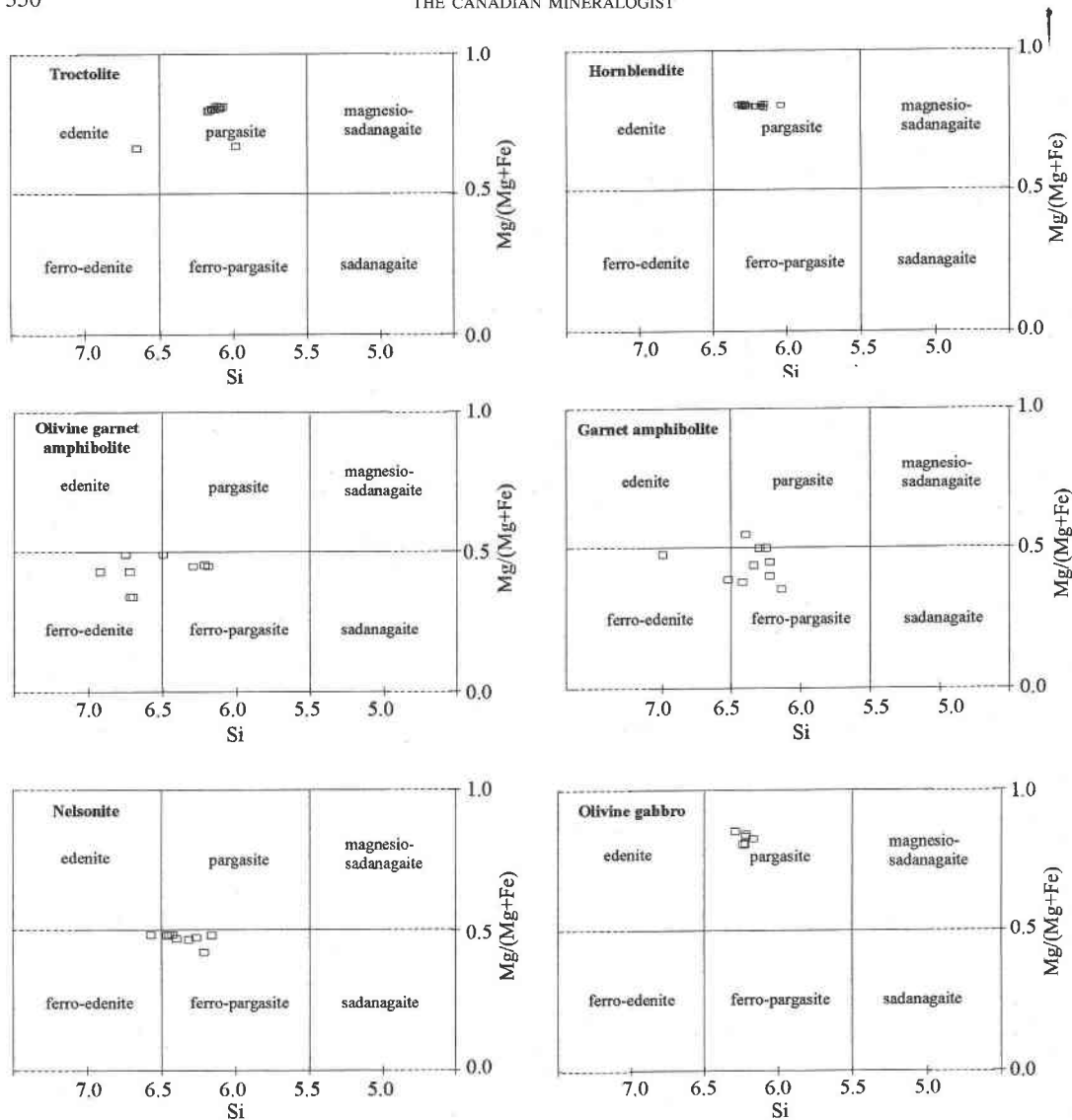


FIG. 9. Ca-amphibole compositions for samples from the Lac Espadon suite. Diagram parameters are $Ca_B \geq 1.50$; $(K+Na)_A \geq 0.50$ and $Ti < 0.50$ (after Leake *et al.* 1997).

calculated using TWEEQU are shown in Table 2 and in Figure 10.

Troctolite (sample 5a)

In the troctolite, the development of a triple corona of orthopyroxene, clinopyroxene and garnet between olivine and plagioclase involves Fe and Mg diffusion from the olivine and Ca and Al diffusion from the plagioclase. For instance, the corona sequence orthopy-

roxene – clinopyroxene – garnet is consistent with higher concentration of Al in the plagioclase domains and higher concentration of Fe and Mg in the olivine domains. Therefore, high Ca and high Mg and Fe in the outer and inner rims of the garnet corona are a direct result of growth in contact with plagioclase and clinopyroxene. The presence of corundum and kyanite inclusions in the plagioclase, on the other hand, is caused by the garnet acting as a buffer for Al (*e.g.*, Yund 1986) leading to an excess of Al in the plagioclase site.

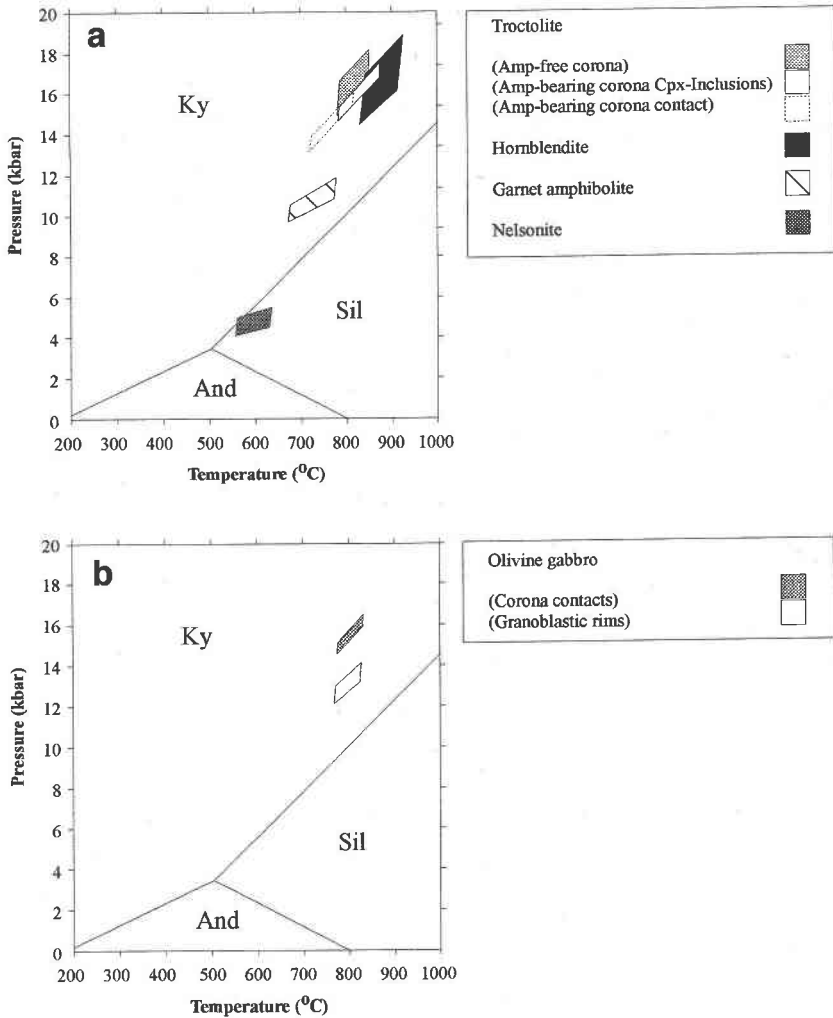
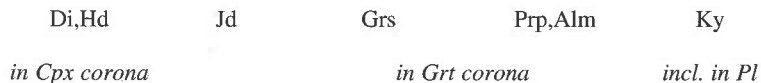
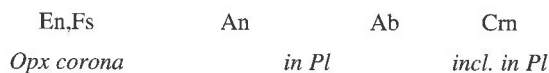
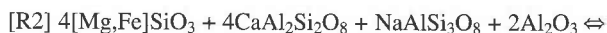


FIG. 10. P-T diagrams showing the maximum and minimum metamorphic conditions calculated partly using the results of analyses in Table 1 for troctolite, hornblende, garnet amphibolite and nelsonite (a) and olivine gabbro (b). The range shown is based typically on 5–20 compositions in total, as well as those in Table 1. All calculations were carried out as independent reactions using the program TWEEQU version 2.02 (Berman 1991), except for garnet–amphibole, which uses version 1.01. P–T estimates quoted are to the nearest 5°C and 0.25 kbars. The results of all P–T calculations are also shown in Table 2.

Thus the development of the triple corona assemblage in a quartz-absent system, along with the presence of corundum and kyanite in the plagioclase, can be represented by the general reactions:



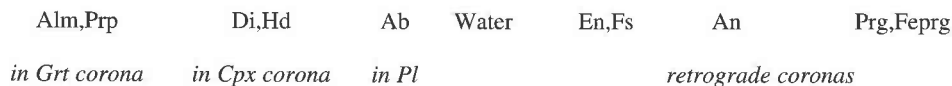
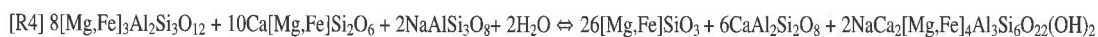
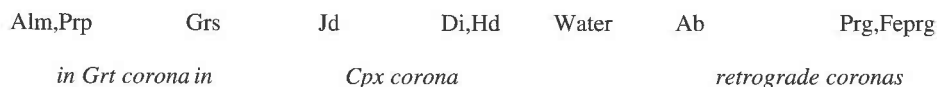
An	Fo, Fa	En, Fs	Grs	Prp, Alm	Crm
<i>in Pl</i>	<i>Ol</i>	<i>Opx corona</i>	<i>in Grt corona</i>		<i>incl. in Pl</i>



In this textural setting, the garnet – plagioclase – kyanite – corundum barometer (Indares & Rivers 1995) can be applied to garnet–plagioclase contacts. The distribution of Fe and Mg between the garnet and clinopyroxene rims can be used to constrain the metamorphic temperatures. The absence of retrograde resetting at both rims of the garnet corona suggests that the equilibrium compositions of the adjacent phases were

achieved during peak-T conditions and are likely preserved (Indares & Rivers 1995). Therefore, calculating P-conditions with garnet compositions at the plagioclase rims and T-conditions at the garnet–clinopyroxene contact should give peak conditions of metamorphism.

The breakdown of the corona assemblage locally to give amphibole and orthopyroxene can be represented by the general reactions:



Reactions [R3] and [R4] require plagioclase among both the reactants and products. Plagioclase is not adjacent to both the garnet and clinopyroxene in the corona assemblage. This fact suggests that some open-system behavior involving fluid is likely responsible for retrogression in the amphibole-bearing corona assemblages. In these coronas, the partial resetting of Ca, Fe and Mg is shown in the zoning profiles of the garnet (Fig. 6b), which is indicative of retrogression. Therefore, the re-equilibration of Fe and Mg between the garnet and orthopyroxene, the garnet and clinopyroxene and the garnet and amphibole may be used to constrain the closure temperature during retrogression. The exchange of Fe and Mg during retrogression may continue at lower-T conditions than reactions involving Ca because of the decoupling of mass transfer and exchange reactions. However, if the recorded temperatures are high (>700°C), then partial resetting of the zoning in Ca at the garnet–plagioclase rims will probably have occurred at the same time as the Fe–Mg exchange (e.g., Cygan & Lasaga 1985, Loomis *et al.* 1985, Chakraborty & Ganguly 1992, Schwandt *et al.* 1996). In this case, the pressure calculated using the garnet – plagioclase – kyanite – corundum reaction at the adjacent rims may be combined with the calculated temperatures to give a

point on the retrograde P–T path. However, the results should be viewed with caution. In addition, comparative estimates of temperature were made using clinopyroxene inclusions in the garnet in the amphibole-bearing corona assemblages.

Peak P–T conditions obtained in amphibole-free coronas with garnet–clinopyroxene corona contacts are in the range 780–870°C at 15.5–18.5 kbar (Fig. 10). In amphibole-bearing coronas, the temperature conditions calculated using garnet–clinopyroxene inclusions give overlapping P–T ranges of 780–880°C at 14.5–17 kbar. However, the retrograded parts of the amphibole-bearing coronas give a lower P–T range of 710–800°C at 13.5–15.75. This is consistent with the development of amphibole or equilibration of this assemblage during cooling. The isopleths defining the reaction are almost identical for both assemblages (Fig. 10) despite the resetting of Ca shown by the garnet in the amphibole-bearing corona. This similarity indicates that cooling was either parallel to the isopleths of reaction during retrogression or that decoupling of mass transfer (P-sensitive) and Fe–Mg exchange (T-sensitive) reactions has occurred.

The temperature ranges calculated using TWEEQU were found to be similar to those calculated using con-

ventional exchange thermometers (Table 2). The garnet–clinopyroxene thermometers of Ellis & Green (1979) and Krogh (1988) gave ranges of temperature overlapping with the TWEEQU approach, although the Krogh (1988) calibration gave slightly lower estimates. The temperatures calculated using orthopyroxene–garnet (Carswell & Harley 1990) and garnet–amphibole (Graham & Powell 1984) also are in general agreement with TWEEQU results.

Hornblende (sample 3b)

Sample 3b displays well-preserved igneous textures such as amphibole oikocrysts and olivine and plagioclase chadacrysts, with garnet coronas around the plagioclase and orthopyroxene coronas around the olivine. Unfortunately, it is not possible to describe the formation of each type of corona with balanced reactions. The abundance of hydrous phases, together with the lack of zoning in the garnet coronas (Fig. 6c), suggest diffusion with some open-system behavior. However, the presence of the garnet – plagioclase – kyanite – corundum assemblage in the plagioclase domains allows pressures to be calculated. Given the evidence of large-scale diffusion in the sample, it is reasonable to combine these estimates of pressure with the temperatures calculated at the adjacent garnet–amphibole contacts and assume that both domains achieved equilibrium at the same thermal conditions, *i.e.*, close to the metamorphic peak or at some early stage of cooling. The P–T conditions recorded by the hornblende are 800–930°C at 14.75–19 kbar (Fig. 10). The garnet–amphibole thermometer of Graham & Powell (1984) also gives ranges of temperature that overlap with the TWEEQU results.

Olivine garnet amphibolite (sample 6am)

Sample 6am is granoblastic; given the extent of metamorphic overprinting, it is not possible to suggest reactions for the development of the main assemblage. The widespread presence of amphibole and orthopyroxene in the matrix does, however, suggest pervasive retrogression, whereas olivine is clearly a relict igneous phase. On the other hand, the presence of abundant inclusions of amphibole in the garnet poikiloblasts suggests that fluid infiltration must have occurred prior to, or during garnet growth. In this rock, garnet cores and olivine compositions were chosen to estimate minimum peak conditions of temperature. In addition, areas with coarse-grained assemblages and straight contacts between the rims of garnet, olivine and orthopyroxene were chosen to determine the temperatures of retrogression or re-equilibration. However, the absence of plagioclase in textural equilibrium with the garnet and matrix minerals prevents an independent estimate of pressure to be calculated for the sample.

Conditions of temperature recorded by garnet cores using garnet–olivine thermometry cover a wide range

between 690–800°C (assuming pressures of 10–12 kbar) and 740–860°C (assuming pressures of 16–18 kbar). Ranges recorded by the garnet rims and adjacent matrix phases are much narrower; they range from 590–670°C for garnet–olivine, and 605–700°C for garnet–orthopyroxene, to 610–720°C for garnet–amphibole exchange (Table 2). The garnet–orthopyroxene thermometer of Carswell & Harley (1990) and garnet–amphibole thermometer of Graham & Powell (1984) give almost identical ranges to those inferred from TWEEQU. However, the estimates of temperature made using the garnet–olivine exchange thermometer of O'Neill & Wood (1980) are about 60°C higher. Overall, the temperatures from the cores are similar to those for the retrograde (amphibole-bearing) coronas in the troctolite, whereas the temperatures recorded by the garnet rims and matrix phases are lower.

Garnet amphibolite (sample 2b)

Like the olivine garnet amphibolite (sample 6am), sample 2b displays a granoblastic texture; it is thus not possible to suggest reactions for the development of the main metamorphic assemblage. The texture revealed by CL images (Figs. 4c, d) suggests the breakdown of the garnet and quartz along with rutile (*i.e.*, high-P assemblage) to form titanite and secondary plagioclase (*i.e.*, low-P assemblage). Garnet zoning also is indicative of retrogression. Given these observations, reactions involving the garnet – amphibole – plagioclase – rutile – titanite – quartz assemblage can be used for calculation of retrograde P–T conditions using garnet rims and adjacent matrix minerals.

The Fe–Mg exchange reaction between garnet and pargasite and a variant of the GRAIL barometer (*e.g.*, Ghent & Stout 1984) were used to estimate the retrograde P–T conditions. The P–T conditions inferred using TWEEQU are estimated at 620–795°C at 9.75–11.75 kbar. The range of temperature given by the Graham & Powell (1984) garnet–amphibole thermometer is almost identical (630–705°C).

Nelsonite (sample 9c)

The nelsonite is markedly higher in Fe and lower in Si (Cox *et al.* 1998) than the other samples and displays distinctive textures. Despite the presence of coronitic textures, high-P minerals other than garnet are absent from the sample. In addition, plagioclase displays spinel inclusions instead of kyanite, probably owing to extensive diffusion of Fe in the plagioclase structure. Garnet compositions are extensively modified by homogenization and partial retrograde resetting. Diffusion rates in plagioclase have been shown to be greatly increased in the presence of F (Snow & Kidman 1991). Thus, the high amounts of apatite (up to 10%) and presumably the high contents of F in the nelsonite may also have contributed to enhanced re-equilibration during cooling.

P–T conditions were calculated using the garnet – plagioclase – spinel – corundum barometer, which has been recently applied in coronitic rocks (Indares & Dunning 1997), and combined with garnet–amphibole exchange thermometry to give the P–T conditions recorded by the sample: 550–690°C and 4–5.5 kbar (Fig. 10). The Graham & Powell (1984) calibration gives lower temperatures (485–560°C). These P–T estimates are interpreted to represent re-equilibration of the textures at some stage on the retrograde path.

Olivine gabbro (sample 35b)

The olivine gabbro displays both coronitic and granoblastic areas, both of which are locally amphibole-bearing. The presence of granoblastic garnet with preserved growth-induced zoning in contact with plagioclase, both of which contain kyanite and corundum inclusions (Fig. 4e), suggests that in places the granoblastic domains escaped retrogression. In these areas, and also in the coronitic domains, reactions [R1] and [R2] can be inferred. In such domains, both granoblastic cores and coronas are likely to preserve high-P conditions. However, only in the coronas where both pressures and temperatures can be measured can thermobarometry be applied to calculate peak P–T conditions. In the granoblastic areas, the garnet rims will tend to re-equilibrate. Retrograde modifications indicated by the presence of amphibole replacing clinopyroxene may be represented by the general reactions [R3] and [R4]. Indeed, the presence of both clear plagioclase and pargasite in the granoblastic rims suggests that these assemblages represent those reactions better than in the troctolite. Thus, the retrograde P–T conditions in this sample can be estimated if we assume that equilibrium was achieved at some point during retrogression. The compositions of plagioclase, garnet and clinopyroxene were measured where all were in contact. However, contacts involving kyanite and corundum in the plagioclase and garnet are sparse, and the effects of secondary reactions involving pargasite and clinopyroxene on the P–T estimates for retrogression in this sample are not known. Thus, the P–T estimates for the conditions of retrogression must be treated with caution.

P–T estimates are 775–870°C at 14.5–16.25 kbar for the corona assemblages and 750–850°C at 12–14 kbar for the retrograded granoblastic assemblages (Fig. 10). Ranges of temperature calculated using TWEEQU and Ellis & Green (1979) closely overlap and are only marginally higher than the Krogh (1988) estimates, and the Graham & Powell (1984) estimates for garnet–amphibole are identical (765–880°C, Table 2).

DISCUSSION AND CONCLUSIONS

The highest P and T conditions are recorded by the amphibole-free coronas in the troctolite (780–870°C at 15.5–18.5 kbar) and the kyanite-bearing garnet coronas

in the adjacent hornblende (800–930°C at 14.75–19 kbar) in the western LES (Fig. 10a). P–T conditions defined by the clinopyroxene inclusions and plagioclase–garnet contacts in the amphibole-bearing coronas overlap those in the amphibole-free coronas and the hornblende (780–870°C at 15.5–18.5 kbar). The preservation of growth zoning in garnet in the amphibole-free coronas of the troctolite suggests that the P–T conditions listed above are those close to the peak conditions of metamorphism. P–T conditions calculated for the garnet amphibolite (620–795°C at 9.75–11.75 kbar) and the nelsonite (550–690°C at 4–5.5 kbar), along with the type of textures and pattern of zoning in garnet, suggest that only retrograde conditions are recorded by these samples. The range in temperature suggested by the garnet contacts (with amphibole, orthopyroxene and clinopyroxene) in the amphibole-bearing coronas in the troctolite (710–800°C) is very similar to that in the garnet amphibolite, whereas the apparent pressures are clearly higher. This pattern suggests that the net-transfer (P-sensitive) reactions involving Ca at the garnet–plagioclase contact closed at higher temperatures than the Fe–Mg exchange at the garnet – clinopyroxene – orthopyroxene – clinopyroxene contacts. Thus, the resultant retrograde P–T point may be erroneous and cannot be used to constrain the P–T path. The interval of temperatures recorded by the olivine garnet amphibolite is more difficult to assess, as no independent pressure could be calculated. However, the highest temperatures recorded by the garnet cores (740–860°C assuming 18 kbar) may represent peak conditions or cooling during the early stages of exhumation. The garnet rim – matrix range of temperature (590–720°C) is clearly lower and probably indicates re-equilibration at amphibolite-facies conditions, as in the case of the garnet amphibolite or nelsonite samples.

In the eastern LES, textural evidence together with local preservation of growth zoning in garnet suggest that part of the assemblage should record conditions close to the peak of metamorphism. The peak P–T conditions obtained (750–870°C at 14.5–16.25 kbar) overlap those in the western LES. The retrograde conditions calculated (750–850°C at 12–14 kbar) overlap those recorded by the amphibole-rich rocks in the western LES, although the range in pressure is slightly higher. Given the evidence from the troctolite that the Ca exchange and Fe–Mg exchange seem to have closed at different times, the same may be the case for the olivine gabbro. However, the retrograde conditions inferred from this sample are recorded by granoblastic rather than coronitic domains. In addition, the sample is not as extensively retrograded as the amphibole-rich samples (garnet amphibolite and nelsonite) from the western LES. Therefore, it is likely that the retrograded domains in the olivine gabbro simply preserve information from a different stage of the P–T path.

The P–T paths are difficult to compare, as there are insufficient data from the eastern LES to fully constrain

the P–T conditions during exhumation. However, the available data suggest that both P–T paths are steep, and compatible with evidence for tectonic exhumation throughout the area (Indares *et al.* 1998). The most extreme conditions recorded in the LES overlap the conditions of metamorphism recorded by the highest structural levels in the underlying Lelukuau terrane (*e.g.*, Indares 1997). Results of U–Pb geochronology constraining the ages of both protoliths and metamorphism show that both units are Labradorian in age and that peak Grenvillian metamorphism occurred in both between *ca.* 1050 and 1040 Ma (Gale *et al.* 1994, Cox *et al.* 1998, Indares *et al.* 1998). The above data support the hypothesis that the LES is a dismembered part of the Lelukuau terrane. Similar P–T conditions (720–825°C at 14–17 kbar) are also recorded by eclogites in the adjacent Baie du Nord segment (Cox & Indares 1999). P–T conditions in the same range and steep P–T paths also characterize eclogite, coronites and amphibolites in the nearby Molson Lake and Gagnon terranes (Rivers & Mengel 1985, Indares 1993, Connelly *et al.* 1995, Indares & Rivers 1995). These studies, along with the data from the LES, indicate a widespread exposure of deep crust in this area of the eastern Grenville Province.

Interestingly, although these rocks record P–T conditions in the eclogite facies field, they have not been transformed into “true” eclogites (Carswell 1990). It is possible that in massive and dry igneous rocks with large grain-sizes, such as the interiors of the LES mafic and ultramafic bodies, reaction rates are slow, resulting in the formation of metamorphic coronas and the preservation of igneous relics (Rubie 1990). Deformed and hydrated rocks, however, allow metamorphic reactions to go to completion during the peak (Austrheim & Griffin 1985, Rubie 1986, Koons *et al.* 1987, Austrheim *et al.* 1997) but are also more prone to retrogression (Heinrich 1982). However, high-P coronites metamorphosed at eclogite facies commonly display omphacitic clinopyroxene (*e.g.*, Mørk 1985, 1986, Indares 1993, Zhang & Liou 1997, Cox & Indares 1999) suggesting “partial” eclogitization. In contrast, the high-P samples in the LES contain clinopyroxene coronas which, although Na-bearing, are not omphacitic. The most likely reason for this is the nature of the protoliths, which are parts of a mafic and ultramafic suite and thus, have low bulk Na-contents.

ACKNOWLEDGEMENTS

This study forms part of the Ph.D. thesis of R. Cox. The authors thank Maggie Piranian, Pam King, and Jeff Saunders for assistance during the microprobe analysis of the samples. Roger Mason and Toby Rivers are gratefully acknowledged for help with the CL microscopy and in revision of the final version of the manuscript. Greg Dunning is thanked for his supervision of R. Cox during the long haul. The authors also gratefully acknowledge Rob Berman and one anonymous reviewer

for detailed and constructive comments, which increased our understanding of the rocks and ultimately improved the final version of the manuscript. Bob Martin also is thanked for his thorough editorial handling of the paper. R Cox was supported by NSERC and Lithoprobe grants during this study.

REFERENCES

- AUSTRHEIM, H., ERAMBERT, M. & ENGVIK, A.K. (1997): Processing of crust in the root of the Caledonian continental collision zone: the role of eclogitization. *Tectonophysics* **273**, 129–153.
- _____ & GRIFFIN, W.L. (1985): Shear deformation and eclogite formation within granulite-facies anorthosites of the Bergen Arcs, western Norway. *Chem. Geol.* **50**, 267–281.
- BERMAN, R.G. (1991): Thermobarometry using multi-equilibrium calculations: a new technique, with petrological applications. *Can. Mineral.* **29**, 833–855.
- _____ & ARANOVICH, L.Y. (1996): Optimized standard state and solution properties of minerals. I. Model calibration for olivine, orthopyroxene, cordierite, garnet and ilmenite in the system FeO–MgO–CaO–Al₂O₃–TiO₂–SiO₂. *Contrib. Mineral. Petrol.* **126**, 1–24.
- CARSWELL, D.A. (1990): Eclogites and the eclogite facies: definitions and classification. In *Eclogite Facies Rocks* (D.A. Carswell, ed.). Blackie and Son Ltd., Glasgow, U.K. (1–13).
- _____ & HARLEY, S.L. (1990): Mineral barometry and thermometry. In *Eclogite Facies Rocks* (D.A. Carswell, ed.). Blackie and Son Ltd., Glasgow, U.K. (83–110).
- CHAKRABORTY, S. & GANGULY, J. (1992): Cation diffusion in aluminosilicate garnets: experimental determination in spessartine–almandine diffusion couples, evaluation of effective binary coefficients, and applications. *Contrib. Mineral. Petrol.* **111**, 74–86.
- CONNELLY, J.N., RIVERS, T. & JAMES, D.T. (1995): Tectonic evolution of the Grenville Province of western Labrador. *Tectonics* **14**, 202–217.
- COX, R., DUNNING, G.R. & INDARES, A. (1998): Petrology and U–Pb geochronology of mafic, high-pressure, metamorphic coronites from the Tshenukutish domain, eastern Grenville Province. *Precambrian Res.* **90**, 59–83.
- _____ & INDARES, A. (1999): Transformation of Fe–Ti gabbro to coronite, eclogite and amphibolite in the Baie du Nord segment, Tshenukutish terrane, eastern Grenville Province. *J. Metamorphic Geol.* (in press).
- CYGAN, R.T. & LASAGA, A.C. (1985): Self-diffusion of magnesium in garnet at 750° to 900°C. *Am. J. Sci.* **285**, 328–350.
- DROOP, G.T.R. (1986): A general equation for estimating Fe³⁺ concentrations in ferromagnesian silicates and oxides from

- microprobe analyses, using stoichiometric criteria. *Mineral. Mag.* **51**, 431-435.
- ELLIS, D.J. & GREEN, D.H. (1979): An experimental study of the effect of Ca upon garnet-clinopyroxene Fe-Mg exchange equilibria. *Contrib. Mineral. Petrol.* **71**, 13-22.
- ENGLAND, P.C. & THOMPSON, A.B. (1984): Pressure - temperature - time paths of regional metamorphism. I. Heat transfer during the evolution of regions of thickened continental crust. *J. Petrol.* **25**, 894-928.
- FUHRMAN, M.L. & LINDSLEY, D.H. (1988): Ternary-feldspar modeling and thermometry. *Am. Mineral.* **73**, 201-215.
- GALE, D., DUNNING, G.R. & INDARES, A. (1994): U/Pb geochronology in the western Manicouagan Shear Belt, Parautochthonous Belt, Eastern Grenville Province. *Abitibi-Grenville Lithoprobe Rep.* **41**, 77-78.
- GHEENT, E.D. & STOUT, M.Z. (1984): TiO₂ activity in metamorphosed pelitic and basic rocks: principles and applications to metamorphism in southeastern Canadian Cordillera. *Contrib. Mineral. Petrol.* **86**, 248-255.
- GRAHAM, C.M. & POWELL, R. (1984): A garnet-hornblende geothermometer: calibration testing and application to the Pelona Schist, southern California. *J. Metamorphic Geol.* **2**, 13-21.
- HARLEY, S.L. & CARSWELL, D.A. (1990): Experimental studies on the stability of eclogite facies mineral parageneses. In *Eclogite Facies Rocks* (D.A. Carswell, ed.). Blackie and Son Ltd., Glasgow, U.K.
- HEINRICH, C.A. (1982): Kyanite-eclogite to amphibolite facies evolution of hydrous mafic and pelitic rocks, Adula Nappe, central Alps. *Contrib. Mineral. Petrol.* **81**, 30-38.
- INDARES, A. (1993): Eclogitized gabbros from the eastern Grenville Province: texture, metamorphic context, and implications. *Can. J. Earth Sci.* **30**, 159-173.
- _____ (1997): Garnet-kyanite clinopyroxenites and garnet-kyanite restites from the Manicouagan Imbricate Zone: a case of high-P - high-T metamorphism in the Grenville Province. *Can. Mineral.* **35**, 1161-1171.
- _____ & DUNNING, G.R. (1997): Coronitic metagabbro and eclogite from the Grenville Province of western Quebec: interpretation of U-Pb geochronology and metamorphism. *Can. J. Earth Sci.* **34**, 891-901.
- _____, _____, COX, R., GALE, D. & CONNELLY, J. (1998): High-PT rocks from the base of thick continental crust: geology and age constraints from the Manicouagan Imbricate Zone, eastern Grenville Province. *Tectonics*, **17**, 426-440.
- _____ & RIVERS, T. (1995): Textures, metamorphic reactions and thermobarometry of eclogitized metagabbros: a Proterozoic example. *Eur. J. Mineral.* **7**, 43-56.
- KOONS, P.O., RUBIE, D.C. & FRUEH-GREEN, G. (1987): The effects of disequilibrium and deformation on the mineralogical evolution of quartz-diorite during metamorphism in the eclogite facies. *J. Petrol.* **29**, 679-700.
- KRETZ, R. (1983): Symbols for rock-forming minerals. *Am. Mineral.* **68**, 277-279.
- KROGH, E.J. (1988): The garnet-clinopyroxene Fe-Mg geothermometer - a reinterpretation of existing experimental data. *Contrib. Mineral. Petrol.* **99**, 44-48.
- LEAKE, B.E., WOOLLEY, A.R., ARPS, C.E.S, BIRCH, W.D., GILBERT, C.M., GRICE, J.D., HAWTHORNE, F.C., KATO, A., KISCH, H.J., KRIVOVICHEV, V.G., LINTHOUT, K., LAIRD, J., MANDARINO, J.A., MARESCH, W.V., NICKEL, E.H., ROCK, N.M.S., SCHUMACHER, J.C., SMITH, D.C., STEPHENSON, N.C.N., UNGARETTI, L., WHITTAKER, E.J.W. & YOUZHI, GUO (1997): Nomenclature of amphiboles: Report of the Subcommittee on Amphiboles of the International Mineralogical Association, Commission on New Minerals and Mineral Names. *Can. Mineral.* **35**, 219-246.
- LOOMIS, T.P., GANGULY, J. & ELPICK, S.C. (1985): Experimental determination of cation diffusivities in aluminosilicate garnets. II. Multi-component simulation and tracer diffusion coefficients. *Contrib. Mineral. Petrol.* **90**, 45-51.
- MÄDER, U.K. & BERMAN, R.G. (1992): Amphibole thermobarometry: a thermodynamic approach. *Geol. Surv. Can., Pap.* **92-1E**, 393-400.
- MARSHALL, D.J. (1988): *Cathodoluminescence of Geological Materials*. Unwin-Hyman, London, U.K.
- MØRK, M.B.E. (1985): Incomplete high P-T metamorphic transitions within the Kvamsøy pyroxenite complex, west Norway: a case study of disequilibrium. *J. Metamorphic Geol.* **3**, 245-264.
- _____ (1986): Coronite and eclogite formation in olivine gabbro (western Norway): reaction paths and garnet zoning. *Mineral. Mag.* **50**, 417-426.
- O'NEILL, H.St.C. & WOOD, B.J. (1980): An experimental study of Fe-Mg partitioning between garnet and olivine and its calibration as a geothermometer. *Contrib. Mineral. Petrol.* **70**, 59-70.
- POGNANTE, U. (1985): Coronitic reactions and ductile shear zones in eclogitized ophiolite metagabbro, western Alps, north Italy. *Chem. Geol.* **50**, 99-109.
- RIVERS, T., MARTIGNOLE, J., GOWER, C.F. & DAVIDSON, A. (1989): New tectonic divisions of the Grenville Province, southeast Canadian Shield. *Tectonics* **8**, 63-84.
- _____ & MENGEL, F.C. (1988): Contrasting assemblages and petrogenetic evolution of corona and non-corona gabbros in the Grenville Province of western Labrador. *Can. J. Earth Sci.* **25**, 1629-1648.

- RUBIE, D.C. (1986): The catalysis of mineral reactions by water and restrictions on the presence of aqueous fluid during metamorphism. *Mineral. Mag.* **50**, 399-415.
- _____ (1990): Role of kinetics in the formation and preservation of eclogites. In *Eclogite Facies Rocks* (D.A. Carswell, ed.), Blackie and Son Ltd., Glasgow, U.K. (111-140).
- SCOTT, D.J. & HYNES, A. (1994): U-Pb geochronology along the Manicouagan corridor, preliminary results: evidence for ca. 1.47 Ga metamorphism. *Abitibi-Grenville Lithoprobe Rep.* **41**, 109-110.
- SCHWANDT, C.S., CYGAN, R.T. & WESTRICH, H.R. (1996): Ca self-diffusion in grossular garnet. *Am. Mineral.* **81**, 448-451.
- SNOW, E. & KIDMAN, S. (1991): Effects of fluorine on solid-state alkali interdiffusion rates in feldspar. *Nature* **349**, 231-233.
- SPEAR, F.S. (1993): Metamorphic Phase Equilibria and Pressure - Temperature - Time Paths. *Mineral. Soc. Am., Monogr.* **1**.
- YUND, R.A. (1986): Interdiffusion of NaSi-CaAl in peristerite. *Phys. Chem. Minerals* **13**, 11-16.
- ZHANG, R.Y. & LIOU, J.G. (1997): Partial transformation of gabbro to coesite-bearing eclogite from Yangkou, the Sulu terrane, eastern China. *J. Metamorphic Geol.* **15**, 183-202.

Received March 24, 1998, revised manuscript accepted March 15, 1999.